Development of Out-of-plane Strengthening System by Passive Compression for Masonry Walls

JUNE 2014

DOCTOR OF ENGINEERING

YULIA HAYATI

TOYOHASHI UNIVERSITY OF TECHNOLOGY

Abstract

Masonry is one of the oldest structural systems and has been widely used over the world even after engineering materials such as concrete and steel had been introduced in construction. Brick masonry is still the most popular building component in developing countries due to its easy handling and cost-effectiveness. Masonry walls typically have low flexural capacities and possess brittle failure modes when exposed to out-of-plane loads.

The current study focuses on improving the out-of-plane performance of masonry walls. Field investigation was conducted on damaged buildings in a central region of Aceh province by the 2013 Aceh, Indonesia earthquake. Building structural systems in the area are roughly classified into four types: 1) reinforced concrete, 2) confined masonry, 3) timber, and 4) timber with masonry spandrel walls. Reinforced concrete and confined masonry suffered from moderate to heavy damage. On the contrary, damage to timber was none to light. The major cause of damage to confined masonry structures was out-of-plane failure of masonry walls. One of the collapsed buildings was focused to evaluate the minimum seismic resistance of masonry walls in the out-of-plane direction. As a result, it was found that the masonry wall collapsed because it could not withstand the intensity of the earthquake that occurred in the area. It shows a need to upgrade the out-of-plane performance of masonry walls to prevent such kind of collapse.

The new out-of-plane loading system for masonry walls is proposed in this study. Uniformly distributed loads are applied to masonry walls by using a rubber airbag. The test system was developed aiming at obtaining basic mechanical characteristics of

simply supported masonry walls in the out-of-plane direction. A test with an aluminum plate specimen was conducted to verify the developed loading system. An easy to handle and lightweight specimen with dimensions of 190 mm x 10 mm for a cross section and a length of 900 mm was used. Consequently, the test results clarified good agreements between the experimental measurements and theoretical estimations.

This study proposes a new out-of-plane strengthening method for masonry walls with passive compression, which is applied to wall cross-section by restraining axial deformation with steel rods. The new strengthening system utilizes geometric deformation characteristics of masonry as well as the mechanism of conventional post-tensioning system. Outer steel rods are provided to apply compression to wall cross-section. Compression is passively induced with geometric axial elongation under out-of-plane loads which is caused by structural characteristics of masonry itself. The strengthening mechanism is implemented to verify its availability. Three brick wall specimens were prepared and tested with/without strengthening with dimensions of 190 mm x 140 mm x 900 mm in width x thickness x length (height). The M8 steel rods which were placed along the wall length and fixed to steel end plates provided on the wall ends are used for strengthening material. As a result, the proposed method significantly improved the structural performance of walls in the out-of-plane direction.

Moreover, a theoretical calculation procedure is presented for the performance evaluation. Verification of the proposed analytical method was conducted through simulating the experimental results of strengthened masonry walls. As a result, good agreements were observed between the experimental and analytical results on the performance evaluation of masonry. Thus, the proposed analytical method can be applied reasonably for estimating the out-of-plane performance of masonry walls strengthened by the proposed method. Moreover, the performance of typical masonry

wall in Aceh was evaluated by applying the proposed analytical method. Finally, it was found that the proposed system can effectively improve the out-of-plane performance of masonry walls.

Acknowledgements

Finally, I would like to thank my beloved son, Hikmatfathiin Aulia, for his unconditional support and encouragement, which has helped me to finish my doctoral program. His love provided me inspiration and the driving force that I needed. Furthermore, this program would not have been completed without the encouragement and affection from my belated parents and my husband (may Allah protect them and place them in heaven). Accordingly, I would like to dedicate this thesis for their pride.

Contents

List of Tables

List of Figures

List of Photos

Chapter 1

Introduction

1.1 Background

Unreinforced masonry (URM) structures are commonly used in building construction throughout the world including in Aceh, Indonesia. Masonry is one of the oldest structural systems and has been widely used over the world even after engineering materials such as concrete and steel had been introduced in construction. Brick masonry is still the most popular building component in developing countries due to its easy handling and cost-effectiveness. Unfortunately, however, no reinforcement is provided in old existing masonry buildings and non-structural masonry components such as exterior/partition walls in developing countries. Such walls are significantly vulnerable to out-of-plane loads which may be caused by seismic action, high speed wind, or blast explosion.

Sumatra Island, Indonesia is located close to a major earthquake fault line, where destructive earthquakes have occurred during the recent years. Moderate shaking by

relatively small earthquakes may not cause many victims, but damage masonry walls in the out-of-plane direction. Such out-of-plane failures of walls indicate a need for strengthening.

Therefore, there have been numerous efforts to upgrade the out-of-plane performance of masonry walls and to develop strengthening schemes. The surface treatment seems to incorporate external reinforcements in some techniques by Hamoush et al. (2001) and Bajpai et al (2003). They applied fiber reinforced polymer overlays and bars, respectively, to upgrade existing masonry walls. On the other hand, the grout and epoxy injection and the confining by R/C tie columns are very conventional techniques for retrofit. Recently, however, Takiyama et al. (2008) proposed developed techniques by inserted stainless pins with epoxy resin in masonry walls to strengthen the out-of-plane performance, and F. Mosele et al (2006) presented new systems which incorporated ties into masonry walls. Moreover, the post-tensioning is an alternative retrofit method which can effectively provide structural stability, as reported by e.g. Ismail et al. (2009). This system is particularly valuable when strengthening historical buildings because it can maintain exterior appearances. However, it generally requires high construction cost, high skills in construction, and maintenance even after constructions, which are not suitable for application in developing countries. Therefore, this study proposes a new post-tensioning system which can reduce specific difficulties in the conventional system.

The new strengthening system utilizes geometric deformation characteristics of masonry as well as mechanism of conventional post-tensioning system. Outer steel rods are provided to apply compression to wall cross-section. Although the conventional post-tensioning system improves sectional performance under previously applied compression, it is not essential to this system. Compression is passively induced with

geometric axial elongation under out-of-plane loads which is caused by structural characteristics of masonry itself. Such strengthening mechanism contributes to reduce specific difficulties in the conventional system.

The objective and outlines of the dissertation are described in the following.

1.2   Research Objective

The major objective of this study is to newly propose out-of-plane strengthening method for masonry walls with passive compression. To reach this objective, in this study, a new out-of-plane loading system was also developed to apply uniform distributed loads to masonry walls by a rubber airbag. The test system was developed aiming at obtaining basic mechanical characteristics of simply supported masonry walls in the out-of-plane direction. Moreover a theoretical calculation procedure is presented for the quantitative out-of-plane performance evaluation for strengthened masonry walls. Several stages of researches are summarized as follows:

1. Field investigation on damage to buildings/housings during the July 2013 Aceh, Indonesia earthquake was carried out after the earthquake event. It was conducted to clarify the major causes of damage to local constructions in Aceh province, Indonesia, and to show the motivation of this research.

2. An out-of-plane loading system was developed to apply it to out-of-plane loading tests of masonry walls. It was essential to investigate static out-of-plane behavior/performance of masonry walls. A verification test of the developed system was also conducted using an elastic plate to show its appropriate action.

3. A new out-of-plane strengthening method was presented in detail. Its effectiveness was verified through comparing the performance of brick wall specimens with/without the proposed strengthening method.

4. A theoretical calculation procedure was proposed for evaluating the out-of-plan performance of masonry walls strengthened by the proposed system. It was presented to realize strengthening design for practical application.

1.3   Dissertation Outline

The dissertation is presented in seven chapters that are organized for following development of an out-of-plane strengthening system. Chapter One introduces the background and objective of this research.

Chapter Two reviews the available literatures regarding to the out-of-plan performance of masonry walls. This chapter also introduces out-of-plan loading system of masonry wall proposed by other researchers.

Chapter Three reports a field investigation in damaged area due to July 2013 Aceh, Indonesia earthquake. The typical constructions and damage in the affected area close to the epicenter is presented in this chapter. An estimation of out-of-plan performance of typical brick masonry walls in this area is also presented.

Chapter Four proposes a new out-of-plane loading system for masonry walls. Its development concept and availability are mentioned in this chapter. A preliminary test using an aluminum plate verifies appropriate action of out-of-plane loads.

Chapter Five proposes a new strengthening system utilizes geometric deformation characteristics of masonry as well as mechanism of conventional post-tensioning system. Compression is passively induced with restraint by outer rods to geometric axial elongation under out-of-plane deformation which is caused by structural characteristics of masonry itself. This chapter also reports the effectiveness through application tests.

Chapter Six presents a theoretical calculation procedure to evaluate the out-of-plane performance of strengthened walls. The proposed analytical model

represents typical behavior of strengthened walls. This chapter also verifies the proposed method comparing with the test results. In addition, this chapter also presents the application of proposed strengthening method to typical walls in Aceh. The conclusions and recommendation for future study regarding to out-of-plane performance of masonry wall structures is finally presented in Chapter Seven.

1.4   References

Bajpai K. and D. Duthinh (2003) "Bending Performance of Masonry Walls Strengthened with Near-surface Mounted FRP Bars", *9th North American Masonry Conference*.

Hamoush S.A, M.W. McGinley, P. Mlakar, D. Scott and K. Murray (2001) "Out-of-plane Strengthening of Masonry Walls with Reinforced Composites", *Journal of Composites for Construction*, Vol. 5, No. 3, pp. 139-145.

Takiyama N, T. Nagae, H. Maeda, M. Kitamura, N. Yoshida and Y. Araki (2008) "Cyclic Out-of-Plane Flexural Behavior of Masonry Walls Rehabilitated by Inserting Stainless Pins", *14th World Conference on Earthquake Engineering*.

F. Mosele, F. Porto, C. Modena, A. Fusco, G. Cesare, G. Vasconcelos, V. Haach, P. Lourenco, I. Beer, U. Schmidt, W. Brameshuber, W. Scheufler, D. Schermer and K. Zirch (2006) "Developing Innovative Systems for Reinforced Masonry Walls", *Diswall project report*, Italy.

Ismail N, Laursen P and Ingham JM (2009) "Out-of-Plane Testing of Seismically Retrofitted URM Walls Using Posttensioning", *Australian Earthquake Engineering Society (AEES) 2009 Conference*.

Chapter 2

Literature Reviews

2.1 Introduction

A masonry wall is wall made from materials which have traditionally been cemented together with the use of mortar. Masonry is one of the oldest structural systems and has been widely used over the world even after engineering materials such as concrete and steel had been introduced in construction. Easy and low-cost constructing is known as a main reason for uses of the brick masonry in the developing countries. Unfortunately, however, no reinforcement is provided in old existing masonry buildings and non-structural masonry components such as exterior/partition walls in developing countries. Such walls are significantly vulnerable to out-of-plane loads which may be caused by seismic action, high speed wind, or blast explosion. Several researchers have been experimentally studied about upgrading the out-of-plane performance of masonry walls and developing the strengthening system.

2.2   Masonry Wall Properties

The masonry is usually made of its unit of clay brick or concrete block, and joint material of mortar which is made of cement, lime, sand and water with varying doses. Consequently, the variety will determine the properties of masonry depending on type of unit and mortar used and also the interface between them. According to Mosalam K. et. al. (2009), the properties of mortar which composed of cement and/or lime, sand and water is varied depending on the proportions. The authors also describe that the interface is the weak link in the system with minimal tensile bond strength and masonry has limited tensile strength. Under tension, tensile failure is characterized by splitting along the interface.

Hendry (2001) describes that the most important properties of masonry unit is compressive strength because of direct relevance to the strength of the wall. The compressive strength obtained apparently depends on dimensions and type of unit. The strength of bricks were up to 100 N/mm^2, however for brick masonry wall have much lower strength or about 20 – 40 N/mm^2. He also describes that the tensile strength of masonry units affects the resistance of masonry under various stress conditions.

As described by Zhimmermann and Strauss (2012), masonry always has to be constructed in bond to guarantee adequate bearing capacity. By placing bricks in an adequate way, a cross bonding through the whole thickness of the wall is achieved. As a result of this, the decisive bond of the bricks depends on the thickness of the wall. Walls with a thickness of the width of a brick were usually built in a stretching bond and walls with a thickness of the length of a brick in a heading bond.

Maidiawati (2013) and Zhimmermann and Strauss (2012) also described that the compressive and tensile strengths affected the structural performance and that the

compressive strength of masonry is higher than tensile strength or flexural strength.

2.3   Out-of-Plane Failure of Masonry Walls

The brick wall is recognized as material with brittle behavior and low resistance to seismic action especially out-of-plane loads. The out-of-plane failure behavior of masonry building has been investigated by some researchers. According to Zhimmermann and Strauss (2012), the flexural loading is a load case which is quite common. As shown in Figure 2.1, when wall is loaded by such as out-of-plane load to its surface then flexural stresses in the perpendicular and the parallel direction of the horizontal joints occur.
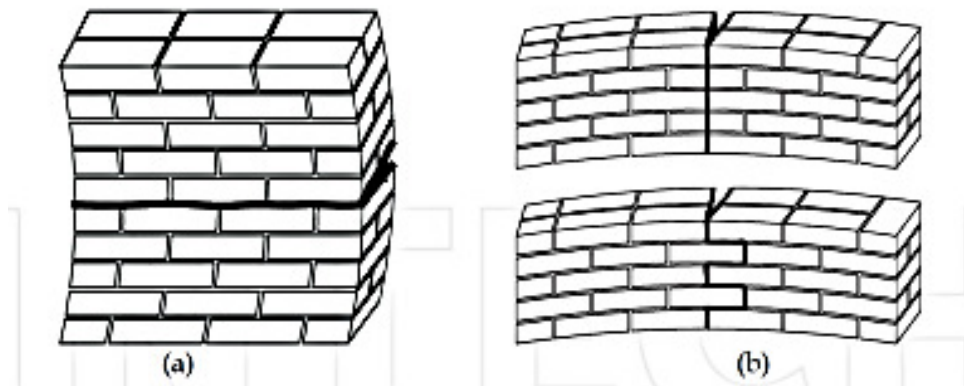
Figure 2.1 Flexural load failure (a) parallel to the horizontal joints and (b) perpendicular to the horizontal joints

Augenti et al. (2013) reported that in May 2012 an magnitude M_L 5.9 earthquake occurred in Emilia Romagna region of Italy. The earthquake caused severe damage to the masonry buildings without RC tie beams in the out-of-plane direction, as shown in Photo 2.1

Photo 2.1 Out-of-plane failure of brick masonry buildings

Figure 2.2 shows that the ground motion is acting transverse to a cantilever or free-standing masonry walls, as report by Arya et al. (2013). The out-of-plane load acting on the mass of the wall tends to overturn it. This wall will collapse as show in Photo 2.2.
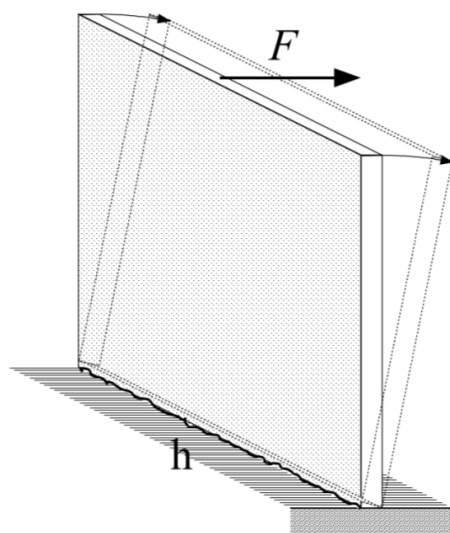
Figure 2.2 Overturning cause by out-of-plane load

1994 Liwa Earthquake, Indonesia   2006 Central Java Earthquake, Indonesia

Photo 2.2 Out-of-plane failure of masonry walls

2.4 Loading Systems for Out-of-plane Experiment

The experimental studies with out-of plane loading systems have been done by several researchers. Shaking tables are usually implemented to investigate out-of-plane performance of unreinforced masonry (URM) walls subjected to inertial forces normal to the surfaces (Mosalam and Hasheni, 2007; ElGawady et. al. 2004 and Yi-Hsuan Tu et al (2010)). It is occasionally difficult to observe failure behavior by optical inspections in dynamic tests.

Ismail et al. (2009), Griffith and Vaculik (2007) and Paulopereira et al. (2011) made a similar test set up for applying out-of-plane load to damaged masonry walls. They used full scale URM wall specimens, as shown in Figure 2.3. In order to have equal pressure and to allow a transmission of a distributed load to the masonry panel, those tests used airbags. All walls were simply supported at top and bottom.
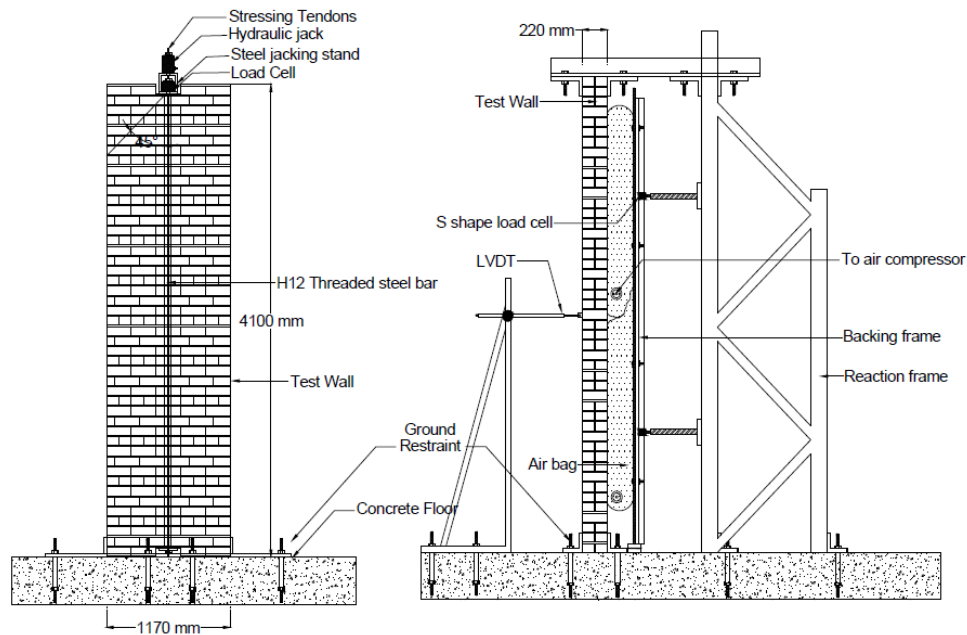
Figure 2.3 Test setup proposed by Ismail et. al. (2009)

However, verification for appropriate loading was not provided in those studies. Therefore, in this study a verification test of the developed system was conducted to obtain more reliable experimental data.

2.5 Strengthening Systems to Upgrade the Out-of-plane performance of Masonry Walls

Masonry walls are significantly vulnerable to out-of-plane loads, however, no reinforcement is provided in old existing masonry buildings and non-structural masonry components such as exterior/partition walls in developing countries. Numerous techniques are introduces by researchers to increase the strength of masonry walls.

ElGawady et al (2004) reviewed typical techniques for retrofitting existing

unreinforced masonry buildings, and categorized into five methods: surface treatment, grout and epoxy injection, external reinforcement, confining by R/C tie columns, and post-tensioning.

The surface treatment seems to incorporate external reinforcements in some techniques by Hamoush et al. (2001) and Bajpai et al (2003). They applied fiber reinforced polymer overlays and bars, respectively, to upgrade existing masonry walls. Figure 2.4 and 2.5 shows their techniques, respectively.
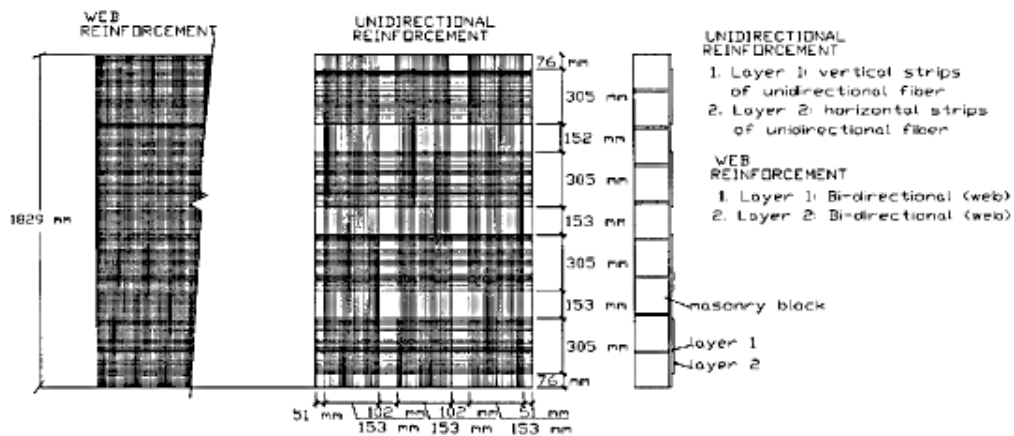
Figure 2.4 Using FRP overlay as external reinforcement techniques by Hamoush et al. (2001)
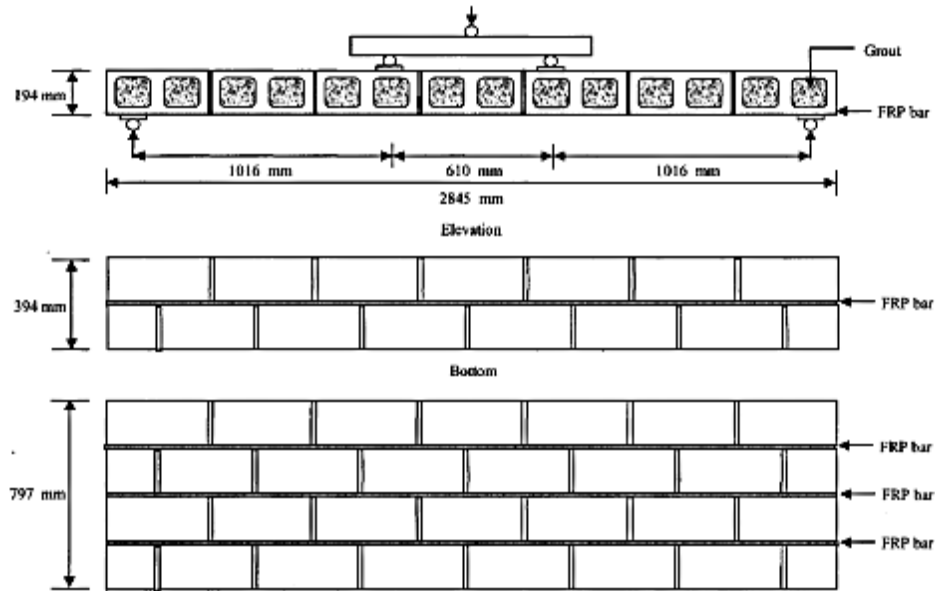
Figure 2.5 Using FRP bar as external reinforcement techniques by Bajpai et al (2003)

On the other hand, the grout and epoxy injection and the confining by R/C tie columns are very conventional techniques for retrofit. As shown in Figure 2.6, Takiyama et al. (2008) proposed developed techniques by inserted stainless pins with epoxy resin in masonry walls to strengthen the out-of-plane performance, and F. Mosele et al (2006) presented new systems which incorporated ties into masonry walls, as shown in Figure 2.7.

(a) Details   (b) Stainless Pins
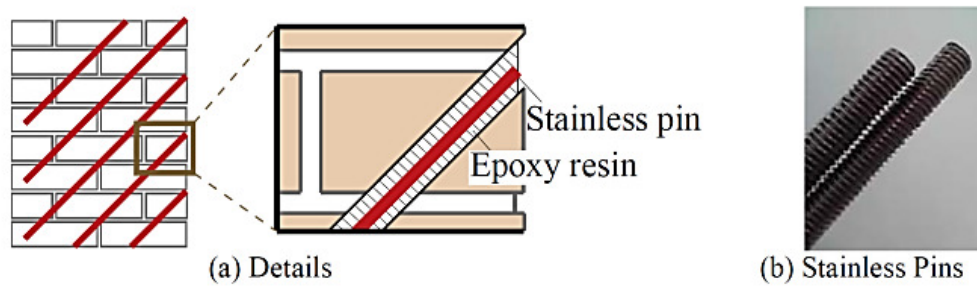
Figure 2.6 Method of inserting stainless pins by Takiyama et al. (2008)
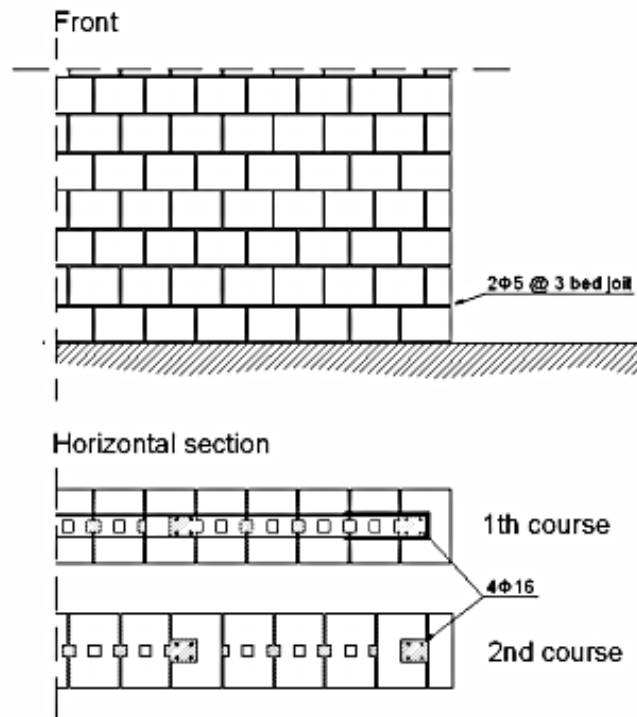
Figure 2.7 Method of incorporated ties into masonry walls by F. Mosele et al (2006)

Post-tensioning involves a compressive force applied to masonry wall; this force counteracts the tensile stresses resulting from lateral loads, as describe by ElGawady et al (2004). Therefore, the post-tensioning is an alternative retrofit method which can

effectively provide structural stability, as reported by e.g. Ismail et al. (2009), as shown in Figure 2.8, respectively. The advantages of this system are to increase the flexural strength and ductility of walls. This system is particularly valuable when strengthening historical buildings because it can maintain exterior appearances. However, it generally requires high construction cost, high skills in construction, and maintenance even after constructions, which are not suitable for application in developing countries. Therefore, this study proposes a new post-tensioning system which can reduce specific difficulties in the conventional system.
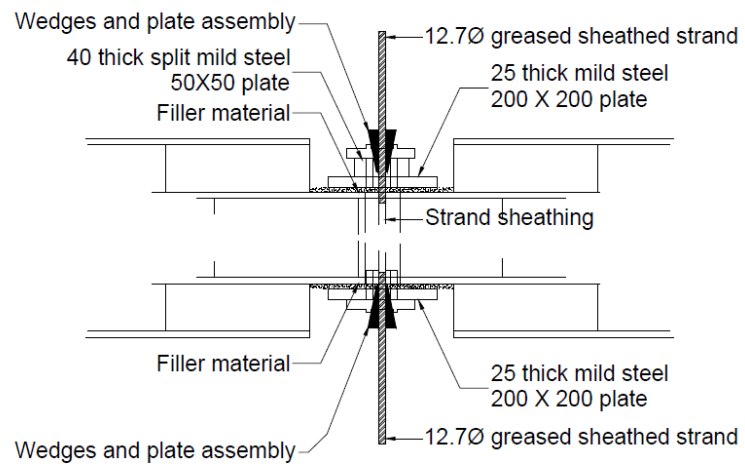
Figure 2.8 Method of post-tensioning system by Ismail et al. (2009)

2.6 Summary

Several past studies developed the experimental methods for out-of-plane loading. Shaking tables are usually implemented to investigate out-of-plane performance of unreinforced masonry (URM) walls for experiment, but it seems occasionally difficult to observe failure behavior by optical inspections during tests. Therefore, this study adopts a simpler test for out-of-plane loading with an air bag for reducing those difficulties. Appropriate action of out-of-plane loads is also verified to obtain relaiable data.

A number of experimental studies have been carried out to introduce strengthening methods to prevent out-of-plane failure. The author focused on the post-tensioning strengthening method considering their logical mechanical mechanism. However, the past systems seem not to be suitable for application in developing countries due to difficulties in construction and maintenance. Therefore, this study proposes a new post-tensioning system which can reduce specific difficulties in the conventional system.

2.7 References

Arya A.S., Boen T. and Ishiyama Y. (2013) "Guideline For Earthquake Resistant Non-engineered Construction", *United Nations Educational, Scientific and Cultural Organization (UNESCO)*.

Augenti N., Nanni A. and Parisi F. (2013) "Construction Failure and Innovative Retrofitting", *Buildings 2013*, Vol. 3, pp. 100-121.

Bajpai K. and D. Duthinh (2003) "Bending Performance of Masonry Walls Strengthened with Near-surface Mounted FRP Bars", *9th North American Masonry Conference*.

ElGawady M, Lestuzzi P and Badoux M (2004) "A Review of Conventional Seismic Retrofitting Techniques for URM", *13th International Brick and Block Masonry Conference.*

F. Mosele, F. Porto, C. Modena, A. Fusco, G. Cesare, G. Vasconcelos, V. Haach, P. Lourenco, I. Beer, U. Schmidt, W. Brameshuber, W. Scheufler, D. Schermer and K. Zirch (2006) "Developing Innovative Systems for Reinforced Masonry Walls", *Diswall project report*, Italy.

Griffith M.C and Vaculik J. (2007) "Out-of-plane Flexural Strength of Unreinforced Clay Brick Masonry Walls", *The Masonry Society Journal*, September, Vol 25, No. 1, pp. 53-68.

Hamoush S.A, M.W. McGinley, P. Mlakar, D. Scott and K. Murray (2001) "Out-of-plane Strengthening of Masonry Walls with Reinforced Composites", *Journal of Composites for Construction*, Vol. 5, No. 3, pp. 139-145.

Hendry E.A.W. (2001) "Masonry Walls: Material and Construction", *Construction and Building Material, Elsevier*, Vol. 15, pp. 323-330.

Ismail N, Laursen P and Ingham JM (2009) "Out-of-Plane Testing of Seismically Retrofitted URM Walls Using Posttensioning", *Australian Earthquake Engineering Society (AEES) 2009 Conference*.

Maidiawati (2013) "Modeling of Brick Masonry Infill for Seismic Performance Evaluation of RC Frame Buildings", *PhD Thesis, Toyohashi University of Technology.*

Mosalam K, and Hashemi A., (2007) "Seismic Evaluation of Reinforced Concrete Buildings Including Effects of Masonry Infill Walls", *Peer Report 2007/100*, Pacific Earthquake Engineering Research Center, University of California, Berkeley.

Mosalam K., Glascoe L., Bernier J. (2009) "Mechanical properties of unreinforced brick masonry." *section 1, LLNL-TR*-417646.

Paulopereira MF, Netopereira MF, Diasferreira JE and Lourenco PB (2011) "Behavior of Masonry Infill Panels in RC Frames Subjected to In Plane And Out Of Plane Loads", *7th International Conference AMCM*, Poland.

Takiyama N, T. Nagae, H. Maeda, M. Kitamura, N. Yoshida and Y. Araki (2008) "Cyclic Out-of-Plane Flexural Behavior of Masonry Walls Rehabilitated by Inserting Stainless Pins", *14th World Conference on Earthquake Engineering*.

Yi-Hsuan Tu, Tsung-Hua Chuang, Pai-Mei Liu and Yuan-Sen Yang (2010) "Out-of-plane Shaking Table Tests on Unreinforced Masonry Panels in RC Frames", *Engineering Structures, Elsevier*, Vol. 32, pp. 3925-3935.

Zhimmerman. T, and Strauss. A. (2012) "Masonry and Earthquakes: Material Properties, Experimental Testing and Design Approaches", *InTech, Europe*.

Chapter 3

Field Investigation on Buildings Damaged during the July 2013 Aceh, Indonesia Earthquake

3.1   Introduction

Aceh province which is located in the northwestern region of Sumatra island, Indonesia is close to a major earthquake fault line, where destructive earthquakes have occurred in recent years. A destructive earthquake with the magnitude 6.1 M_L occurred in central region of Aceh province about 181 km southeast from the capital of Banda Aceh, as shown in Figure 3.1.

Aceh Tengah and Bener Meriah districts suffered moderate damage due to the earthquake. The authors investigated damage to buildings and houses around Takengon city which is the capital city of Aceh Tengah district and mountain areas close to the epicenter of earthquake for obtaining the specific data on local constructions and their damage. Figure 3.2 shows the survey route map from Banda Aceh to the affected areas.

In particular, an inventory survey was conducted at Ratawali village, which is located about 11 km east from the epicenter, to clarify major causes of the damage. This chapter reports the results of on-site investigation.

3.2   Description of the Earthquake

According to U.S Geological Survey (USGS) (USGS, 2013), the epicenter of magnitude 6.1 M_L earthquake, occurred at 14:37 (local time in Indonesia) on July 2, 2013 was located at 4.698^0N, 96.687^0E with a depth of 10 km, as shown in Figure 3.1.

Based on reports by the United Nations Children's Fund (UNICEF) Indonesia (Unicef, 2013), the earthquake affected Aceh Tengah and Bener Meriah districts. Table 3.1 shows the summary of earthquake disasters in Aceh Tengah and Bener Meriah districts, respectively. Completely collapsed houses were observed at several villages close to the epicenter, while Takengon, the capital of Aceh Tengah district about 20 km southeast from the epicenter, did not suffer serious damage, as shown in Photo 3.1.
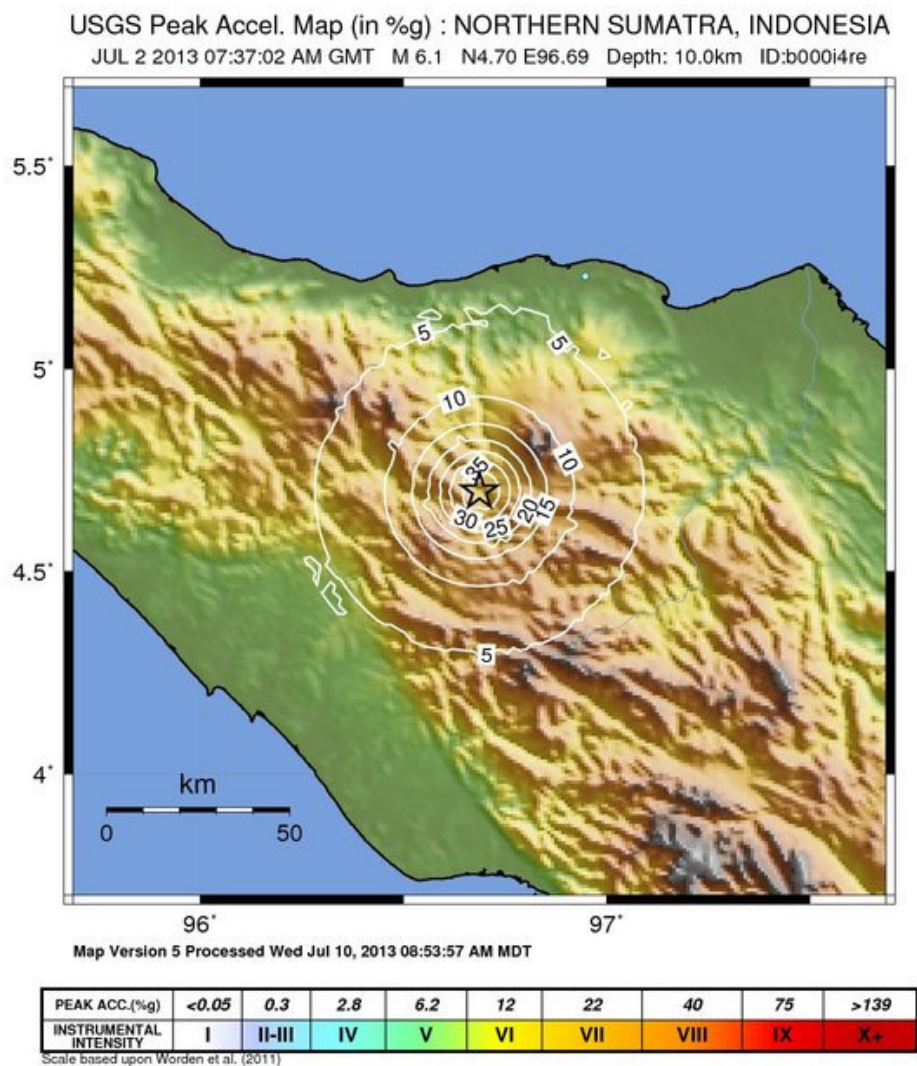
Figure 3.1 Epicenter of 6.1 M_L earthquake shake map (USGS, 2013)

Table 3.1. Earthquake disaster summary

Information	Aceh Tengah district	Bener Meriah district
Killed victim	31 persons	8 persons
Injured victim	2418 persons	114 persons
Affected villages	79.69%	49.36%

(a) Overall route map

(b) Investigated area

Figure 3.2 Survey route map of investigation (Google Earth)

(a) Serempah on the epicenter

(b) Ratawali village at about 11 km from the epicenter

(c) Takengon

Photo 3.1 Investigated area

3.3   Typical Constructions and Damage

The first stage of investigation was a preliminary damage survey in Takengon and mountain areas close to Serempah village on the epicenter of earthquake to observe typical buildings/housings and their damage. Figure 3.2 shows the survey route map from Banda Aceh to the affected area. Photo 3.1 shows the condition around Takengon city and mountain areas close to the epicenter of earthquake.

Building/housing structural systems can be roughly classified into four types: 1) Reinforced Concrete (RC), 2) Confined Masonry (CM), 3) Timber (T), and 4) Timber with Masonry spandrel wall (T+M), as shown in Photo 3.2. The last three types were typical structures at villages in the mountain range close to the epicenter.

(a) Reinforced concrete

(b) Confined masonry

(c) Timber

(d) Timber with masonry spandrel wall

Photo 3.2 Typical structures at earthquake-damaged area

Photo 3.2a shows an example of typical RC buildings whose major damage was observed to non-structural masonry walls as well as structural columns. Severe damage to non-structural walls prevented RC buildings from immediate occupancy, as shown in Photo 3.3. CM houses consist of brick walls with slender RC tie columns/beams, which are provided along the perimeters of masonry walls, and a wooden/aluminum roof truss with tiles/zinc plates or an RC roof slab, as shown in Photo 3.2b. This type of construction suffered moderate to heavy damage, such as: complete collapse, collapse

of confining elements, out-of-plane failure of walls, etc., as shown in Photo 3.4. Photo 3.2c and 3.2d show T and T+M houses, respectively. These constructions consist of wooden walls and a roof made of tiles/zinc plates, while T+M construction has brick spandrel walls under wooden walls. Damage to these systems were generally lighter, however some of them leaned due to ground settlement or damage to masonry spandrel walls, as shown in Photo 3.5.

Photo 3.3 Damage to non-structural walls in RC buildings preventing immediate

occupancy

(a) Complete collapse

(b) Collapse of confining element

(c) Out-of-plane failure of gable wall

(d) Out-of-plane failure of wall

Photo 3.4 Typical damage to confined masonry

(a) T house damaged due to ground
settlement

(b) T+M house leaning with failure
of masonry spandrel walls

Photo 3.5 Damage to timber

3.4 Statistical Investigation Results

An inventory survey was conducted at Ratawali village 11 km far from the epicenter, as shown in Figure 3.2b. In this small village, 64 samples of affected structures were inspected along the main street, as shown in Figure 3.3. Figure 3.4 compares the number of samples among four construction types. CM and T types covered 45% of total samples, respectively. On the other hand, only one RC and five T+M samples were obtained at the area.
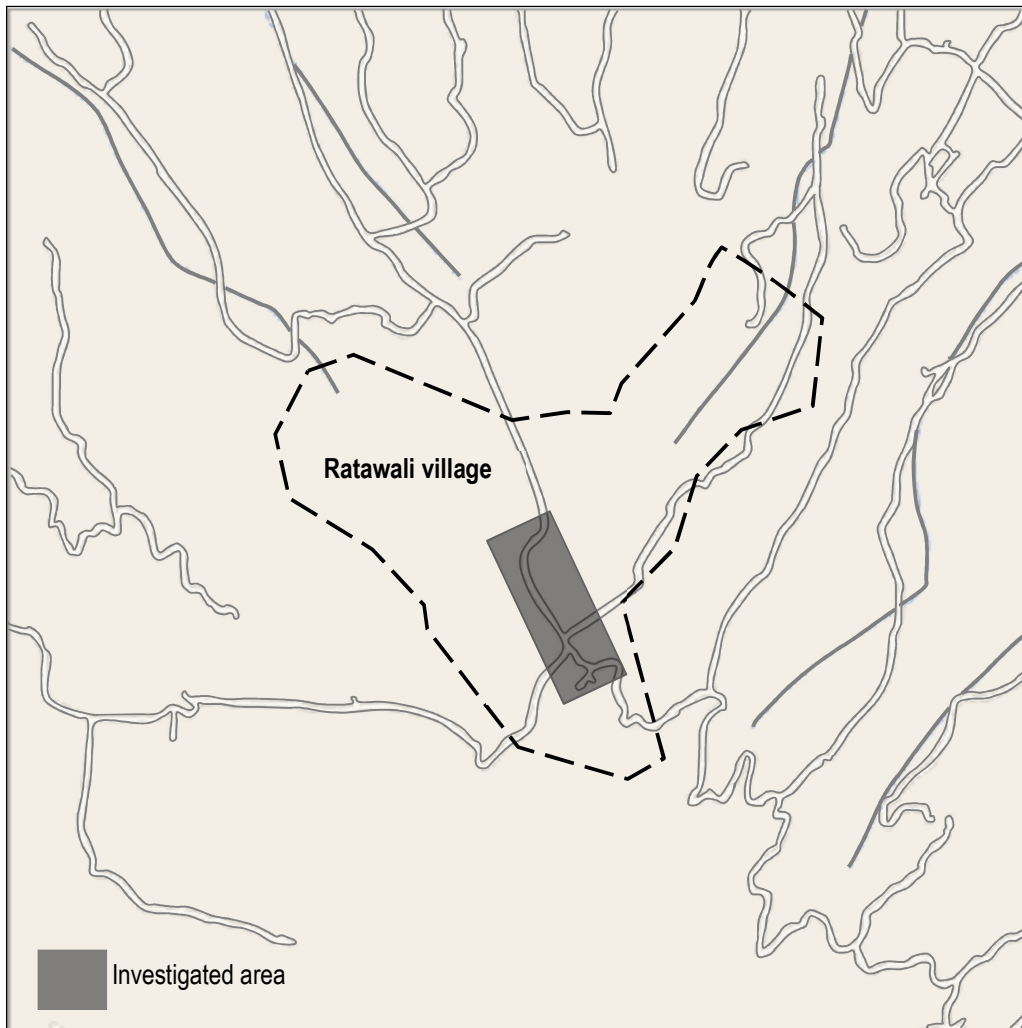
a) Investigated area in Ratawali village
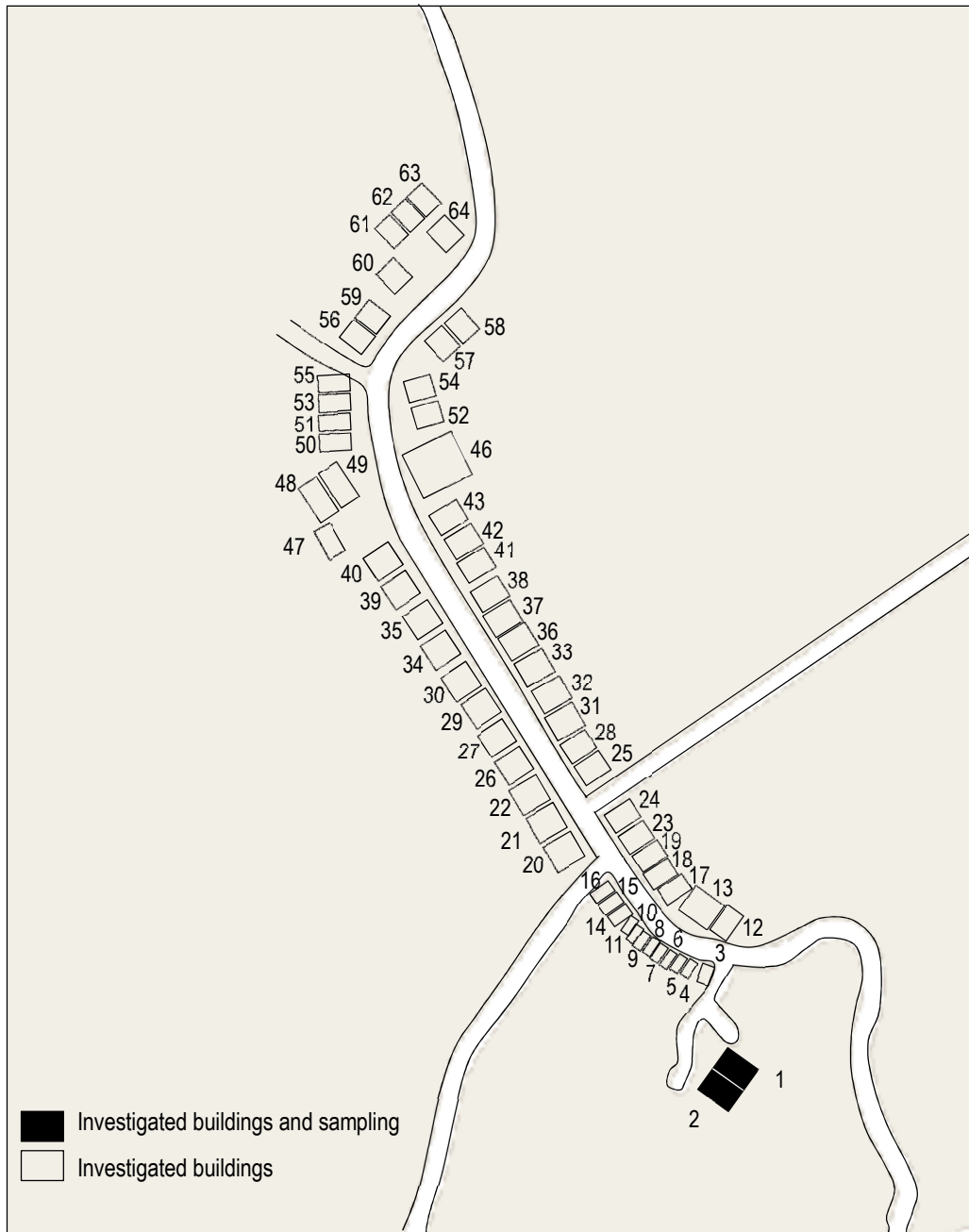
b) Locations of investigated housings/buildings

Figure 3.3 Samples for quantitative investigation
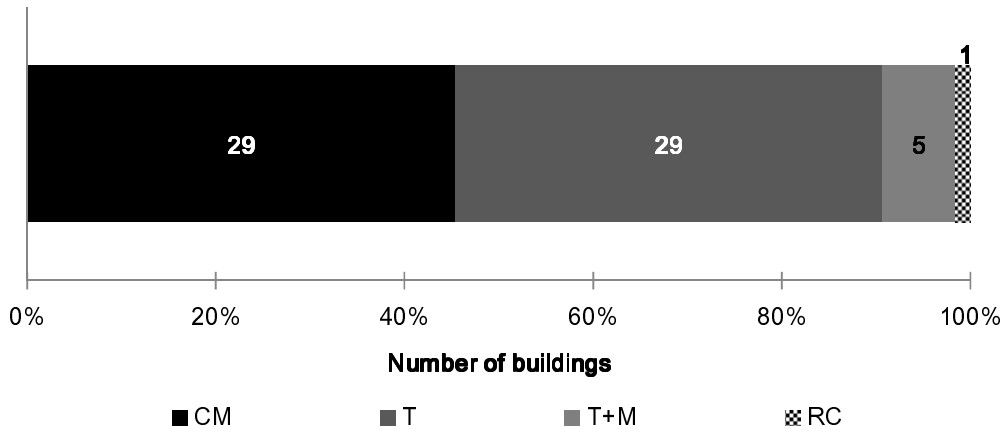
Figure 3.4 Structural systems at the investigated area
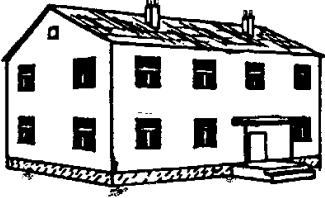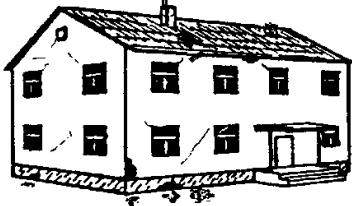
3.4.1 RC and CM Type Buildings

Damage to RC and CM structures was classified into five grades based on European Macroseismic Scale 1998 (EMS-98) (Grunthal. G, 1998). Table 3.2 summarizes the damage classification for masonry buildings by EMS-98 and Photo 3.6 gives samples of the damage grades for CM structures. Figure 3.5 shows the distributions of damage grade for RC and CM constructions. Only one sample of RC building was categorized into Grade 4 due to severe damage to columns, as shown in Photo 3.7, according to EMS-98 in which heavy structural/non-structural damage was defined as Grade 4.   Total 29 CM structures suffered severe damage: Grades 5 and 4 for 62% and 24% of the total, respectively.

Subsequently, Photo 3.9 summarizes typical damage to masonry walls. In addition to categorize the damage, Figure 3.6 gives the ratio of such wall damage types: out-of-plane failure, leaning, shear cracking, and separation between wall and boundary elements. Out-of-plane failure and leaning of walls were clearly caused by out-of-plane loads and generally lead higher damage grades of V to III. On the other hand, walls with

shear/separation cracks were judged into smaller grades of II to I, which might be caused by in-plane loads. Only two samples were obtained for the latter case according to the investigation results. Moreover, complete collapses with damage grade of V also seemed to be related to out-of-plane failure of walls, while it is impossible to identify particular causes of collapses. Therefore, it seems that upgrading the out-of-plane performance of masonry walls is essential to effectively reduce severe damage to masonry structures.

Table 3.2 Damage grade classification for masonry buildings according to EMS-98

	Grade 1: Negligible to slight damage (no structural damage, slight non-structural damage) Hair-line cracks in very few walls. Fall of small pieces of plaster only. Fall of loose stones from upper parts of buildings in very few cases.
	Grade 2: Moderate damage (slight structural damage, moderate non-structural damage) Cracks in many walls. Fall of fairly large pieces of plaster. Partial collapse of chimneys.
	Grade 3: Substantial to heavy damage (moderate structural damage, heavy non-structural damage) Large and extensive cracks in most walls. Roof tile detach. Chimneys fracture at the roof line; failure of individual non-structural elements (partitions, gable walls)
	Grade 4: Very heavy damage (heavy structural damage, very heavy non-structural damage) Serious failure of walls; partial structural failure of roofs and floors.
	Grade 5: Destruction (very heavy structural damage) Total or near total collapse.
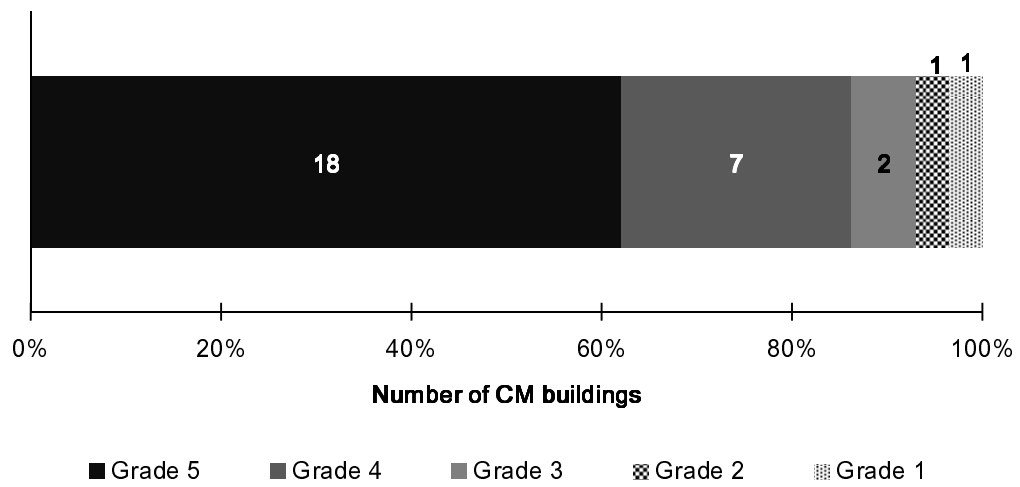
Figure 3.5   Distributions of damage grade for CM constructions

Grade 1   Grade 2

Grade 3

Grade 4

Grade 5

Photo 3.6 Examples of damage grades of CM structures

Photo 3.7 Damaged RC structure

Number of CM buildings

- ■ Complete collapse by unknown reason (V)
- ■ Out-of-plane failure (IV & V)
- ■ Leaning of wall (III & IV)
- ▨ Shear cracks on wall (II)
- ▨ Separation between wall & boundary elements (I)

* number of out-of-plane failure of gable ( )
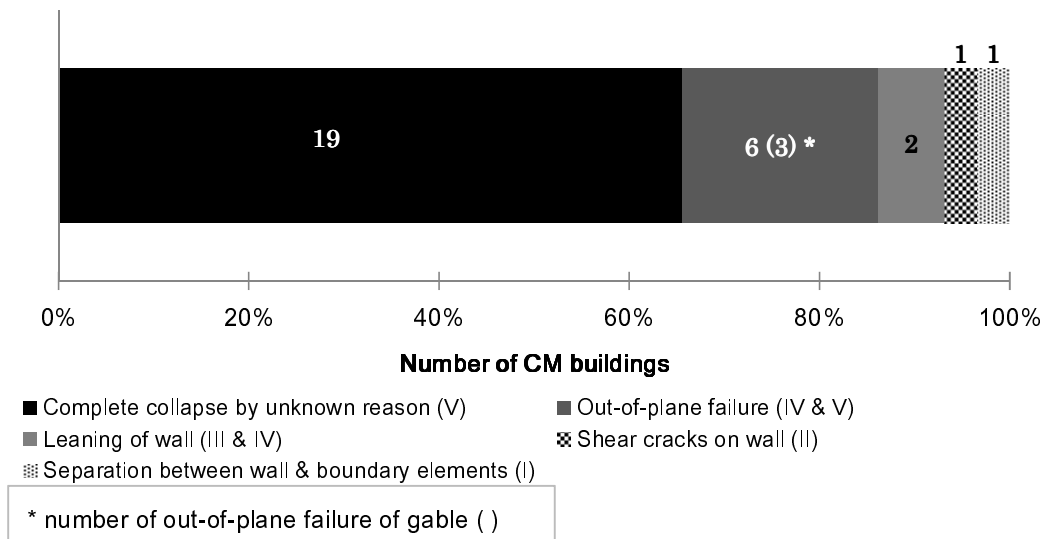
Figure 3.6 Distributions of wall damage pattern for CM constructions

Separation between wall and column

Leaning of wall

Shear crack on wall

Out-of-plane failure of gable wall

Out-of-plane failure of wall

Photo 3.8 Examples of wall damage to CM structures

3.4.2 T and T+M Type Buildings

On the other hand, damage grades for T and T+M constructions were classified into three grades based on the authors' visual observations to typical damage, as shown in Table 3.3. Damage grades for T and T+M constructions are exemplified in Photo 3.9, and their distributions are compared in Figure 3.7.

Total 29 timber houses showed the lowest damage: no damage to light damage for 83% of the total. Only very few cases suffered moderate damage such as titling with about 3^0-4^0, heavy damage such as large titling and total collapse, i.e. 7% and 3% of the total, respectively. Meanwhile, 40% of total 5 timber with masonry spandrel wall houses suffered crack on masonry and spalling of plaster as moderate damage and another 40% of total suffered total collapse which was caused by spandrel wall failure, except for 20% of total or one house with no damage.

Table 3.3 Damage grade classification for timber constructions with/without masonry spandrel walls

Grade	Description	
	T	T+M
I	No damages to light damage	No damage to light damage
II	Moderate damage with titling under 4^0	Moderate damage with crack and fall of several pieces of plaster
III	Collapse	Collapse
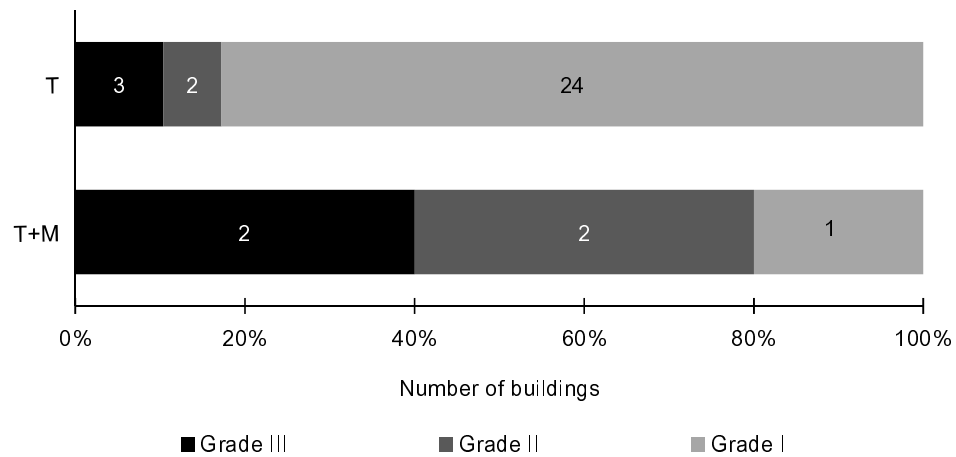
Figure 3.7 Distributions of damage grade for T and T+M constructions

Grade 1 for T

Grade 1 for T+M

Grade 2 for T

Grade 2 for T+M

Grade 3 for T

Grade 3 for T+M

Photo 3.9 Examples of damage grades of T and T+M structures

3.5   Estimation of Out-of-Plane Performance of Typical Brick Masonry Walls

Typical brick masonry walls which are used in Aceh have dimensions of about 4000 mm width x 3000 mm height in local construction such as store, houses and small offices, with 250 kg/m^2 weight per wall area, as shown in Figure 3.8. This section provides a brief estimation of out-of-plane performance of the wall.
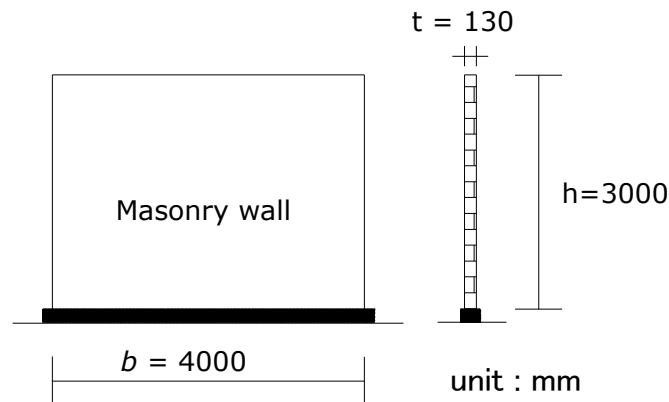
Figure 3.8 Structural dimensions of typical brick masonry wall

One of the collapsed buildings which was located in Ratawali village, as shown in Photo 3.10, was focused to evaluate the seismic resitance of masonry walls in the out-of-plane direction. Based on the on-site inspection and interviews with the occupants, this single-story of simple masonry building was built in 1986 and used for an elementary school building. Some masonry rubbles were collected and transported to Syiah Kuala University to carry out laboratory tests to obtain the material properties. The rubbles were cut to the dimensiones of 180 mm x 130 mm x   200 mm and 200 mm x 130 mm x 280 mm in width x thickness x height for compression and bending tests, respectively, as shown in Photo 3.11.

Photo 3.10 Collapsed elementary school building

Photo 3.11 Cutting specimens for tests

As a result of the compression test, the averaged compressive strength in the longitudinal direction of prism specimens was 2.83 N/mm^2. The tensile strength was obtained by three point load tests, as shown in Photo 3.12. The averaged value was 0.40 N/mm^2 according to Eq. 3.1.
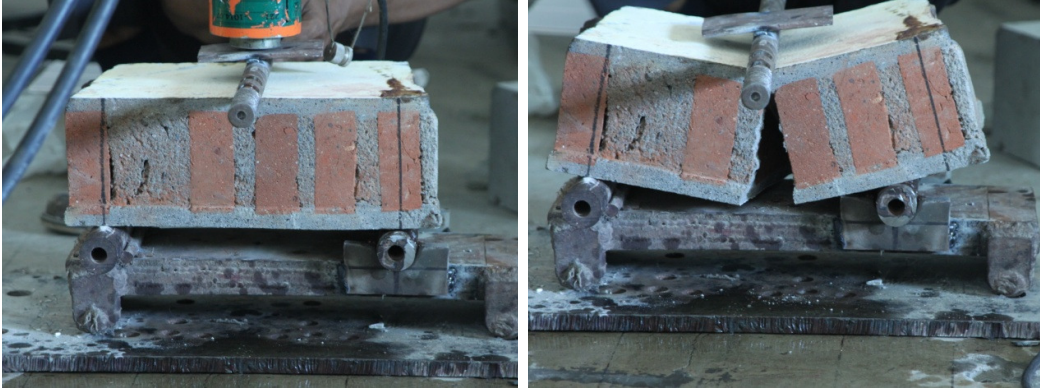
Photo 3.12 Bending test

$$\sigma = \frac{M\,y}{I} = \frac{M}{Z} \qquad\qquad (3.1)$$

where, σ: tensile strength, M: maximum moment under three point loads, y: distance from neutral axis to outer surface, I: moment of inertia, Z: section mudulus $(= \frac{b\,d^2}{6})$.

The axial stress is evaluated by Eq. 3.2 and the value was 0.05 N/mm^2.

$$\sigma_0 = \frac{W}{b\,t} \qquad\qquad (3.2)$$

where, W: weight of wall, σ_0: axial stress, b: width of wall, t: thickness of wall.

The maximum moment for a cantilever wall under a uniform distribution load in the out-of-plane direction, w is evaluated by Eq. 3.3. Substituting Eq 3.3 for M in Eq. 3.1, the applied distribution load and total load carried by the wall were obtained by Eqs. 3.4 and 3.5, respectively.

$$M = \frac{w\,l^2}{2} \qquad\qquad (3.3)$$

$$w = \frac{2 \, \sigma \, Z}{l^2} \tag{3.4}$$

$$F = w \cdot l \tag{3.5}$$

where, w: distribution load, σ: total strength, l: height of wall, F: load-carrying capacity of wall.

The acceleration converted from the load as follows:

$$F = \frac{W}{G} A, \;\; so \;\; A = \frac{F}{W} G \tag{3.6}$$

where,

F: load carrying capacity of wall = 3421.98 N

W: weight of wall = 29419.95 N p d

G: gravity acceleration = 9.8 m/s^2

A : equivalent acceleration = 1.1 m/s^2

As a result, it was found that the specimen might fail under an acceleration of 0.11 g. Based on the information on shakemap in Figure 3.1, the maximum intensity estimated by USGS (2013) for the site is about 0.24 g, which means that the acceleration estimated from the calculation above is less than the USGS estimation. It can be concluded that the masonry wall did not have enough strength to prevent the out-of-plane failure.

3.6   Summary

1. Structural systems can be classified into four types: 1) Reinforced Concrete, 2) Confined Masonry, 3) Timber, and 4) Timber with masonry spandrel wall in the affected area by the 2013 Aceh, Indonesia earthquake.

2. Reinforced concrete and confined masonry structures suffered from the moderate to heavy damage/total collapse.

3. On the contrary, no damage to light damage was observed in timber structures and those with masonry spandrel walls.

4. Damage to CM structures was caused mainly by out-of-plane loads, which resulted in out-of-plane failure and/or leaning of masonry walls.

5. Typical masonry walls in local construction seemed to fail under an acceleration of 0.11 G which means that masonry walls suffered out-of-plane failure because it could not withstand the intensity of the earthquake that occured in the area.

3.7   References

http://unicefindonesia.blogspot.jp/2013/07/after-earthquake-in-aceh-indonesia.html

Grunthal G. (1998) "European Macroseismic Scale 1998", Conseil de L'Europe Cahiers du Centre Europeen de Geodynamique et de Seismologie, Luxembourg, 1998.

USGS website: http://www.usgs.gov/

Chapter 4

Development of Loading System for Out-of-plane Test on Masonry Walls

4.1 Introduction

This chapter proposes a new out-of-plane loading system for masonry walls. Uniform distributed loads are applied to masonry walls by a rubber airbag. The test system was developed aiming at obtaining basic mechanical characteristics of simply supported masonry walls in the out-of-plane direction. In this study, a structural test was conducted to verify the developed loading system by using an aluminum plate specimen. As the result, the test results clarified good agreements between the experimental measurements and theoretical estimations.

Although shaking tables are usually implemented to investigate out-of-plane performance of unreinforced masonry (URM) walls subjected to inertial forces normal

to the surfaces (Mosalam and Hasheni, 2007 and ElGawady et. al. 2004), it is occasionally difficult to observe failure behavior by optical inspections in dynamic tests. Therefore, this study proposes a new static loading system which was developed with a rubber airbag, and implemented for evaluating out-of-plane performance of URM walls. A verification test of this developed system was conducted to obtain more reliable experimental data by using an elastic specimen.

4.2   Design of Loading System

Photo 4.1 shows an out-of-plane loading system for URM walls developed in this study. Design details of the system can be referred to Figure 4.1. A rubber bag jack (airbag), as shown in Photo 4.2, was adopted as a generator for uniform distributed loads normal to wall surfaces. Internal pressure in the airbag was generated by a widely used air compressor. The detailed information of rubber airbag is shown in Table 4.1. The airbag was placed between the reaction frame, which consisted of H-shaped steel and was anchored on a reaction floor, and prospective specimens, as shown in Photo 4.1 and Figure 4.1. Specimens were inserted below the airbag and simply supported in the system. Applied loads to specimens which resulted from the airbag were measured by load cells implemented under the roller supports.
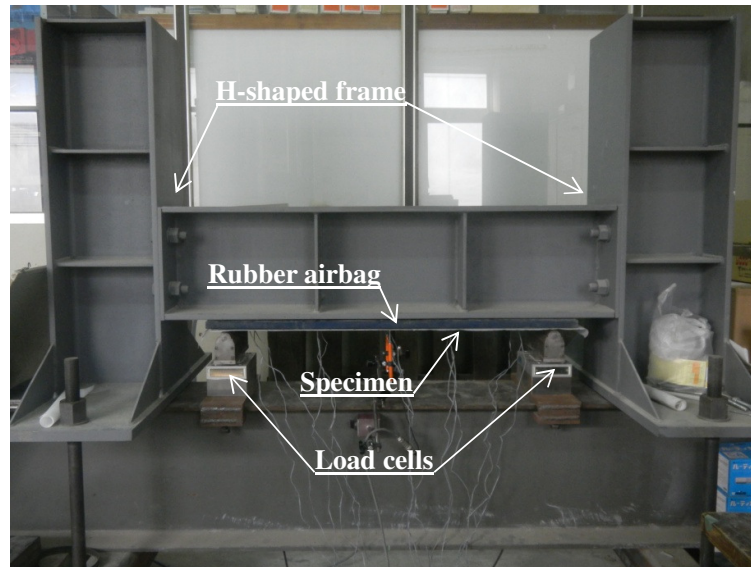
Photo 4.1   Front View of Out-of-Plane Loading System
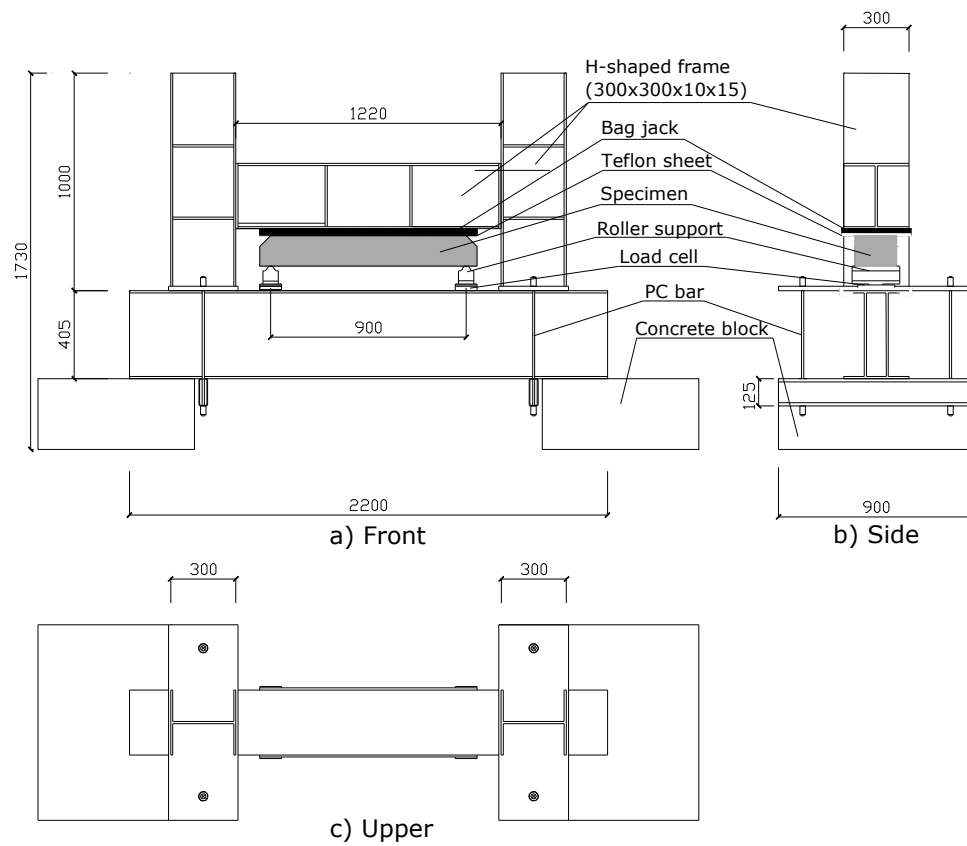
Figure 4.1   Design Details of Out-of-Plane Loading System
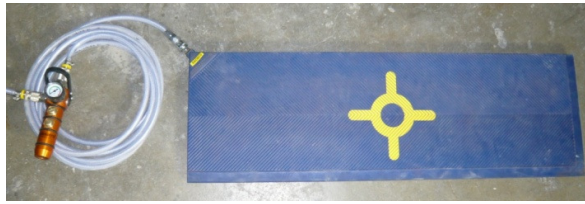
a) Before pump by air compressor

b) After pump by air compressor

Photo 4.2   Implemented Airbag

Table 4.1   Airbag details

Dimension	
Length (mm)	319.0
Width (mm)	1000.0
Thick, before pump (mm)	25.0
Thick, after pump (mm)	215.0
Maximum capacity (kN)	240.0
Maximum pressure (Mpa)	0.8

4.3   Verification of Loading System

4.3.1   Specimen for Verification

An aluminum plate specimen as shown in Photo 4.3 was prepared for a verification test of out-of-plane loading system. The aluminum specimen had enough strength for the verification test, therefore, it was chosen considering its ease to handle because of the light weight. In particular, appropriate action of uniform distributed loads

was verified through comparing experimental results with theoretical calculations. Table 4.2 shows the material properties of aluminum. Figure 4.2 illustrates locations of strain gauges/displacement transducers installed on the bottom surface/side faces of the specimen. In particular, output of each strain gauge means an extreme fiber strain on the tension side when loads were applied by the airbag.
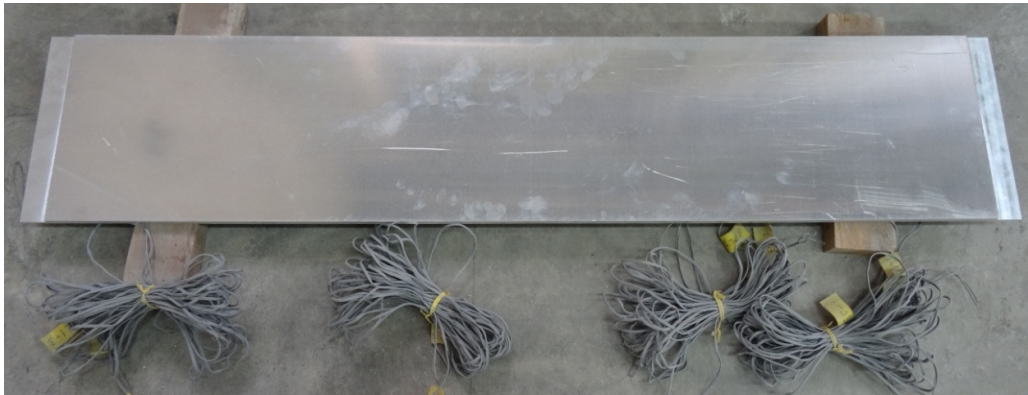
Photo 4.3   Aluminum plate specimen

Table 4.2   Material properties of aluminum

Dimension	
Length (mm)	900.0
Width (mm)	190.0
Height (mm)	10.0
Yield strength (N/mm^2)	98.0
Young modulus (N/mm^2)	62.6 x 10^3
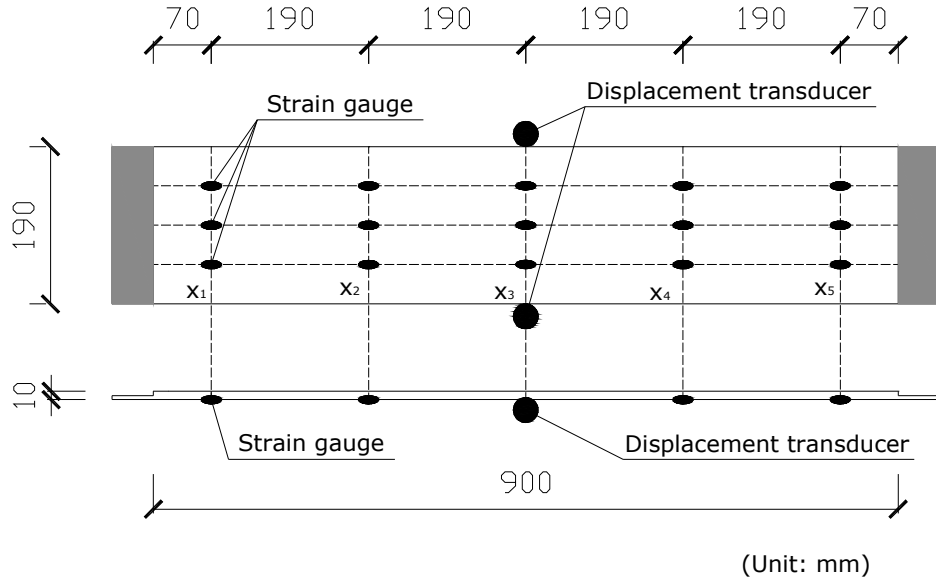
Figure 4.2　Measurements location on/beside the elastic specimen.

4.3.2 Verification Results

Static monotonic loading was applied to the elastic specimen to compare the experimental results with theoretical calculations. In the following comparisons, a theoretical vertical deformation δ at the middle span and strain ε_x along the x-axis were obtained by:

[δ at the middle span]

$$\delta = \frac{5 \cdot w \cdot l^4}{384 \cdot E \cdot I} = \frac{5 \cdot P \cdot l^3}{384 \cdot E \cdot I} \qquad (4.1)$$

where, w: distribution load, l: span length, E: Young's modulus, I: moment of inertia, P: total vertical load ($= wl$)

50

[ε_x along the x-axis]

$$\varepsilon_x = \frac{M_x}{Z\,E}\ ,where\ \ M_x = \frac{wl}{2}\,x - wx\,\frac{x}{2}$$

$$= \frac{1}{2}\,(wlx - wx^2)$$

$$So,\quad \varepsilon_x = \frac{(wlx - wx^2)}{2ZE}$$

$$= \frac{\left(Px - \frac{P}{l}x^2\right)}{2ZE} \tag{4.2}$$

where, M_x: moment along the x-axis, Z: modulus of section.

Figure 4.3a shows the relationship between applied load and vertical deformation at the middle span, where the experimental deformation is the averaged value of outputs from two transducers shown in Figure 4.2. Figure 4.3b shows a transition of the distributions of experimental strains, which represent the moment distributions, along the plate length under several loads indicated in Figure 4.3a. However, the experimental strain at each location means the averaged value of three measurements along the width of specimen, as shown in Figure 4.2. It was found that symmetric distributions were observed throughout the test. Moreover, in these figures, theoretical calculations are compared to the experimental results. Good agreements were observed between the experimental and theoretical values, which mean that the proposed out-of-plane loading system successfully subjected the specimen to uniform distributed loads.
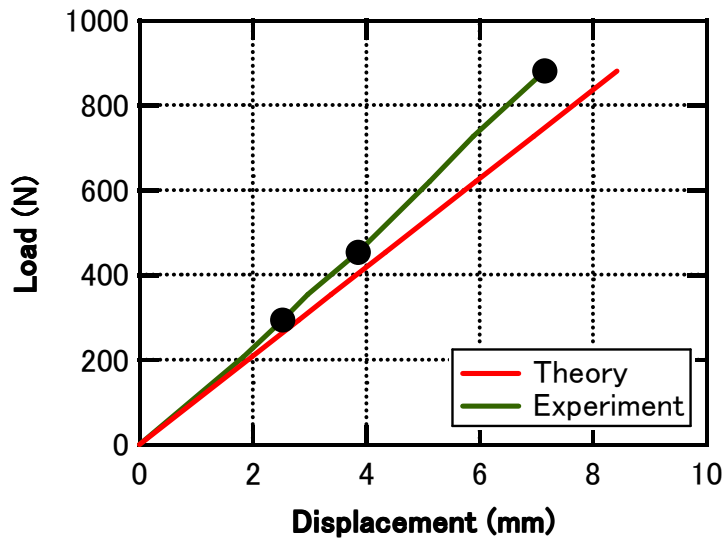
(a) Comparison of load-deformation relationships
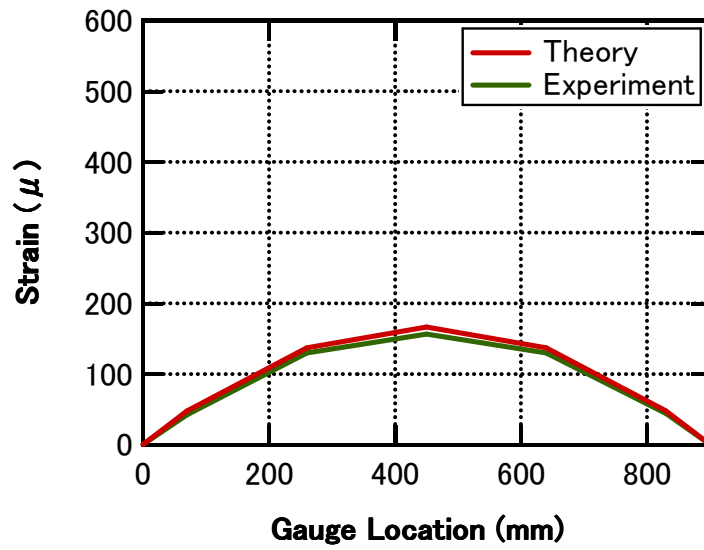
Load of 0.29 kN
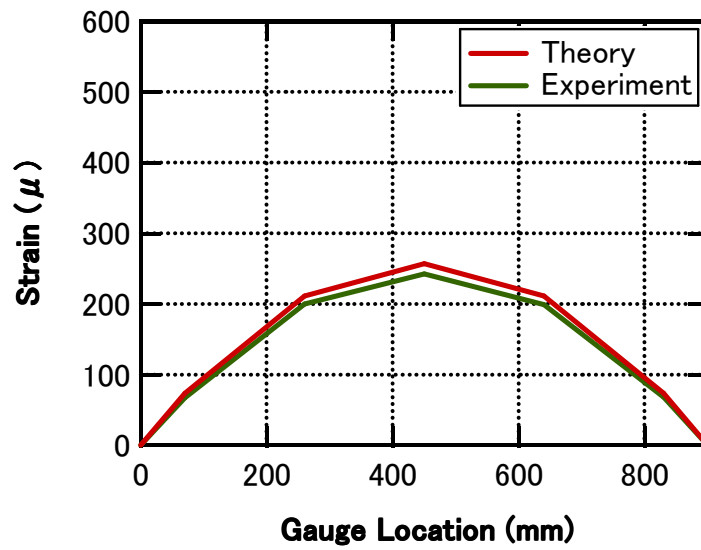
Load of 0.45 kN
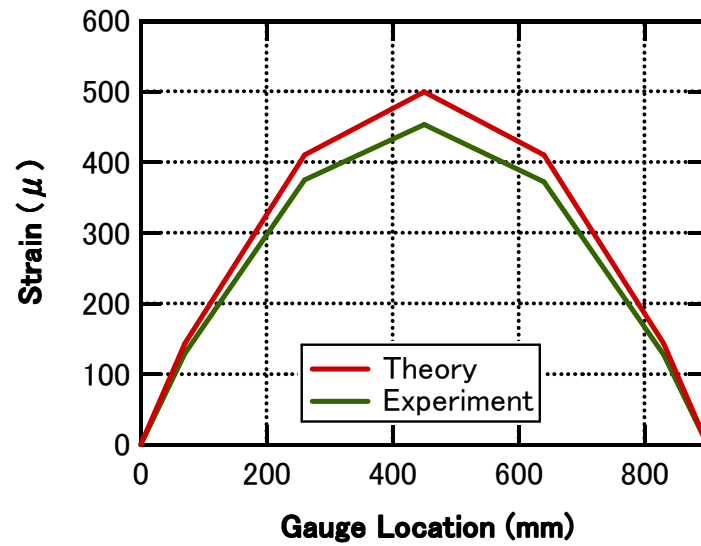
Load of 0.88 kN

(b) Comparisons of strain distributions

Figure 4.3   Comparisons between experimental and theoretical results.

4.4 Summary

- A new out-of-plane loading system was developed by using a rubber airbag for evaluating structural performance of masonry walls in the out-of-plane direction.

- Uniformly distributed loads can be applied to prospective specimens, which was verified through a preliminary test with an elastic plate. Good agreements were obtaned between the experimental measurements and theoretical caluculations.

4.5 References

ElGawady M, Lestuzzi P and Badoux M (2004) "A Review of Conventional Seismic Retrofitting Techniques for URM", *13th International Brick and Block Masonry Conference.*

Mosalam K, and Hashemi A., (2007) "Seismic Evaluation of Reinforced Concrete Buildings Including Effects of Masonry Infill Walls", *Peer Report 2007/100*, Pacific Earthquake Engineering Research Center, University of California, Berkeley.

Chapter 5

Proposal of Out-of-Plane Strengthening Method by Passive Compression for Masonry Walls

5.1   Introduction

Several systems have been introduced to strengthen the out-of-plane performance of masonry walls. Post-tensioning is one of retrofit methods which can effectively provide structural stability (Ismail et al., 2009). This system is particularly valuable when strengthening historical buildings because it can maintain exterior appearances. However, it generally requires high construction cost, high skills in construction, and maintenance even after constructions, which are not suitable for application in developing countries. Therefore, this study proposes a new post-tensioning system which can reduce specific difficulties in the conventional system, as mentioned below.

The new strengthening system utilizes geometric deformation characteristics of

masonry as well as mechanism of conventional post-tensioning system. Outer steel rods are provided to apply compression to wall cross-section. Although the conventional post-tensioning system improves sectional performance under previously applied compression, it is not essential to this system. Compression is passively induced with geometric axial elongation under out-of-plane loads which is caused by structural characteristics of masonry itself. Such strengthening mechanism is described in detail in this chapter.

The major objectives of this study are to introduce the strengthening mechanism and to verify the proposed system through a series of laboratory tests.

5.2   Proposal of Strengthening Method

Masonry walls are commonly fragile in the out-of-plane direction when subjected to lateral loads caused by earthquake, wind, or blast. This is because of low tensile/bond strength of masonry units/adhesive. Therefore, applying compression e.g. due to pre-stressing or post-tensioning is effective to improve the out-of-plane performance (Ismail, et al., 2009). On the other hand, masonry units and typical adhesive of cement mortar can resist high compression. Such characteristics of masonry materials cause geometric axial elongation of walls with lateral deformation under out-of-plane loads, as illustrated in Figure 5.1(a).

Focusing on the specific characteristics of masonry walls, this study proposes a new strengthening system which utilizes the geometric axial elongation above. The strengthening is implemented by providing outer steel rods which restrain the geometric elongation of wall and passively generate axial compression on the wall cross-section as a reaction of restraint, as shown in Figure 5.1(b). Therefore, no previous stress is

necessarily provided for the wall cross-section as well as restraint rods in the proposed system, which results in preventing/reducing complexity in construction, long-term pre-stress loss, and maintenance after construction.
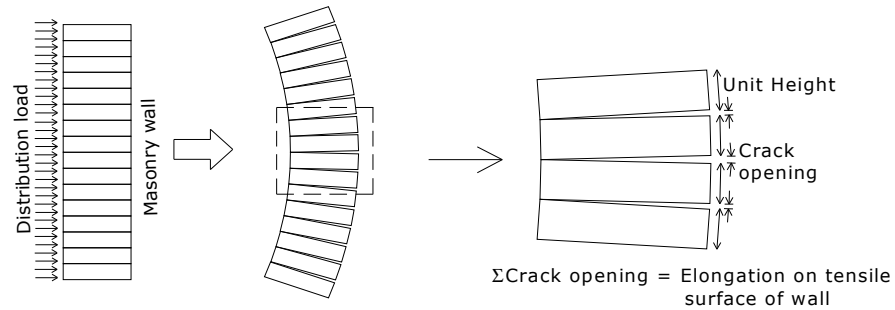
(a) Geometric elongation of masonry walls
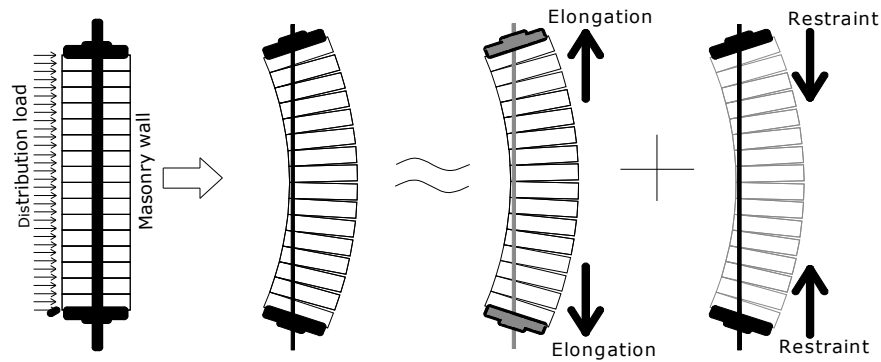
(b) Proposal of restraint system

Figure 5.1 Concept of retrofitting

A series of feasibility tests was conducted to verify the effectiveness of the proposed strengthening system using typical brick walls in Indonesia in the following.

5.3   Experiments for Verification

Earthquake-damaged reinforced concrete (R/C) buildings were investigated after the 2007 Sumatera earthquakes by Maidiawati and Sanada (2008). The investigation focused on two similar buildings: totally collapsed and moderately damaged ones. Specimens for a series of verification tests were obtained from the surviving building as follows.

5.3.1 Specimens and Measurements

The proposed strengthening method was applied to brick wall specimens which were extracted from an earthquake-damaged building in Indonesia and transported to Japan from Indonesia, as shown in Photo 5.1.

Three brick wall specimens were prepared with the dimensions of 190 mm x 140 mm x 900 mm in width x thickness x length (height), as shown in Photo 5.2 and Table 5.1. Young's modulus and compressive strength in the longitudinal direction of the specimens are 1.93 kN/mm^2 and 2.91 N/mm^2, respectively, as shown in Table 5.2. The stress-strain relationships from compression tests on prism specimens are shown in Figure 5.2(a).

One of the specimens was the control specimen, N, which was not strengthened. The other two specimens of S and SI were strengthened by M8 steel rods which were placed along the wall length and fixed to steel end plates provided at the wall ends, as shown in Photo 5.3 and Figure 5.3. Initial tensile strains were applied only to the rods of the SI specimen to induce initial compression on the cross-section, while no pre-stressing was provided for the S specimen. The cross-sectional area, Young's modulus, and yield strength of the rods are shown in Table 5.2, respectively. The

stress-strain relationships from tensile tests of steel rods are shown in Figure 5.2(b).

Photo 5.1 Moderately Damaged Building and Preparing the Brick Masonry Specimens

Photo 5.2 Brick Masonry Specimens

Table 5.1 Experimental parameters

Specimen	N	S	SI
Strengthening*	N	S	S
Loading method**	D	D	D
Initial strain***	0	0	400

* N: none, S: strengthened.
** D: uniformly distributed load
*** Unit: μ.

Table 5.2 Material properties of specimens

Specimen	N	S	SI
Brick Wall			
Young's modulus (kN/mm^2)	1.93	1.93	1.93
Compressive strength (N/mm^2)	2.91	2.91	2.91
Steel Rods			
Cross-sectional area (mm^2)	-	36.6	36.6
Young's modulus (kN/mm^2)	-	229	229
Yield stress (N/mm^2)	-	560	560
Tensile strength (N/mm^2)	-	838	838
Initial strain*/stress** (μ / N/mm^2)	-	0/0	400/0.25

 * tensile strain of rod.
** compressive stress on wall cross-section.
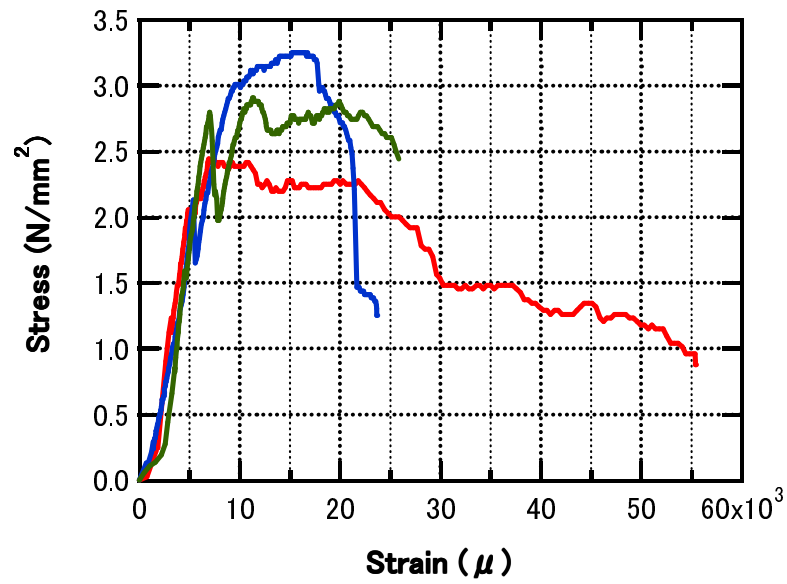
a) Compression test results of prism specimens of brick walls
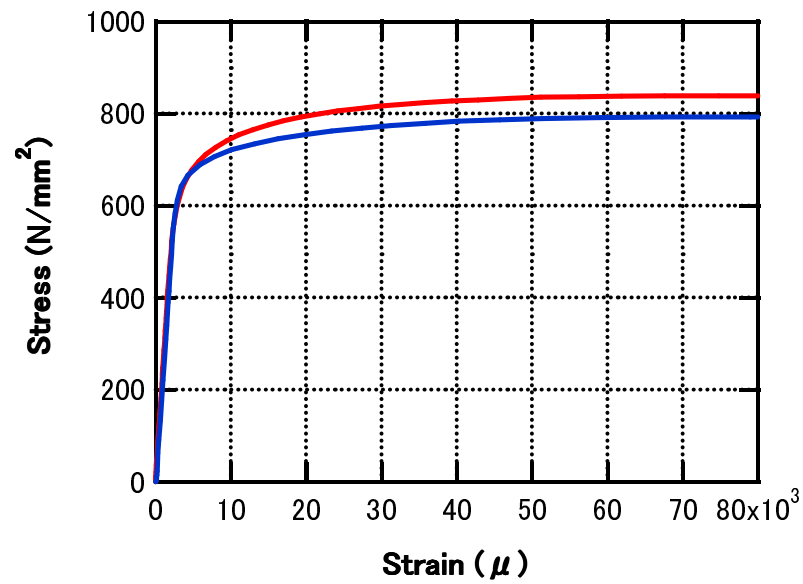
b) Tensile test results of rods

Figure 5.2 Stress-strain relationships from material tests
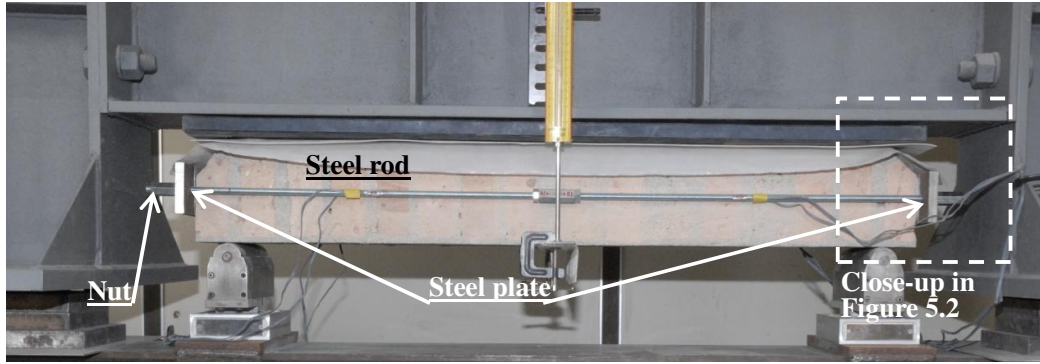
Photo 5.3 Brick wall specimen strengthened by steel rods

(a) Close-up of wall end in Photo 5.1   (b) Side view
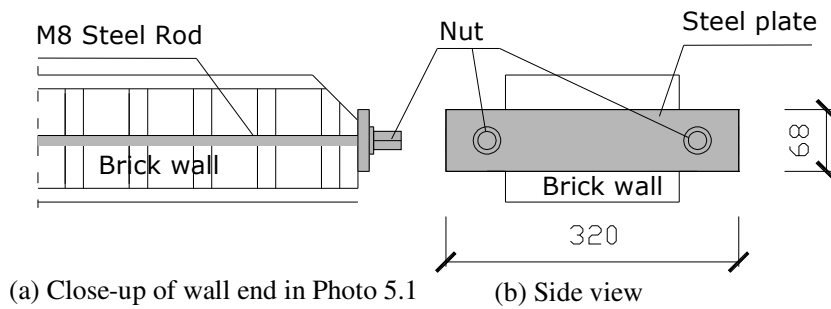
Figure 5.3 Details of end plate

5.3.2   Experimental Methods

Photo 5.4 shows the out-of-plane loading system, which was developed in Chapter 4, to apply uniformly distributed loads to the specimens. Details of the system can be referred to Figure 4.1. A rubber bag jack (airbag) was adopted as a generator for uniform distributed loads normal to wall surfaces, and placed under the steel reaction beam. The specimens were horizontally inserted below the airbag and simply supported in the system. Applied loads to the specimens which resulted from the airbag were measured by load cells implemented under the supports. Set-up of measurements for the tests can be seen in Figure 5.4. Vertical deformations were measured at the middle span of the specimens. The figure also shows locations of strain gauges on the steel rods of the strengthened specimens, which were installed to measure tension of strengthening

rods and resultant compression acted on the wall cross-sections. Initiated cracks were optically observed to identify the failure mechanisms.
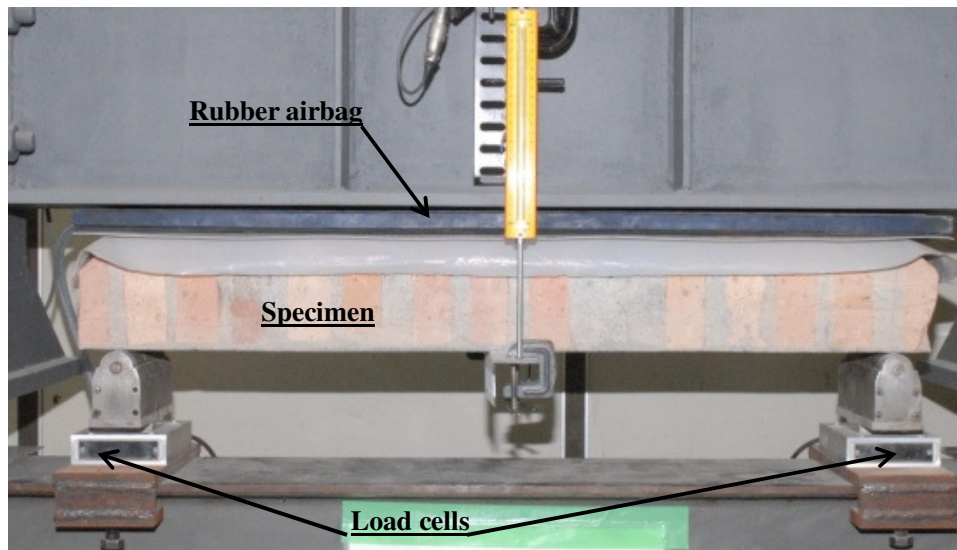
Photo 5.4 Front view of out-of-plane loading system
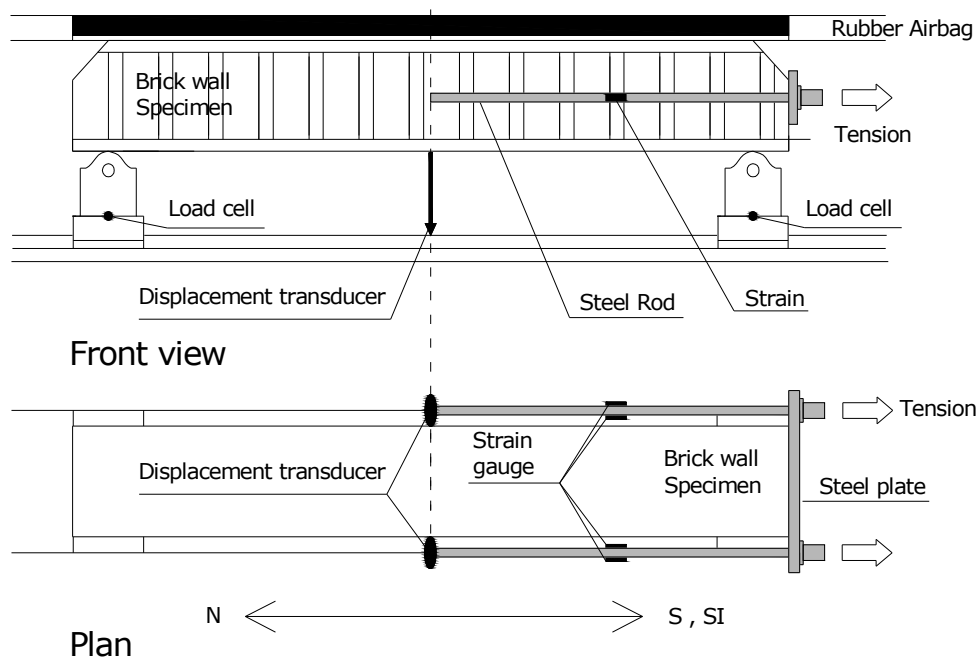
Figure 5.4 Test set-up

5.4 Experimental Results

Figure 5.5 compares the relationships between external moment and drift angle at the middle span between the strengthened and unstrengthned specimens, respectively. However, the external moment was evaluated by Eq. 5.2, and the drift angle was defined dividing the vertical deformation by half of the wall length.

$$M_e = \frac{ql^2}{8} = \frac{Pl}{8} \tag{5.2}$$

where, M_e: external moment, P: total load, l: wall length, q: uniformly distributed load.

Although the N specimen failed under a small moment of 158 Nm at an initial cracking, the strengthened specimens exhibited much higher resistances even after cracking. Photo 5.5 shows the specimens after cracking. It is found that the strengthened specimens sustained out-of-plane loads after a flexural crack occurred and opened. Flexural cracks caused 50 to 150 mm away from the middle span because moment gradients are relatively shallow around the middle span under distribution loads. The drift angles at the maximum moments were around 3.0% rad. for the strengthened specimens. On the other hand, the N specimen failed at a small drift angle of 0.05% rad.

Moreover, in the cases of strengthened specimens, the external moments are also compared to the internal resistances evaluated by Eq. 5.3 in Figure. 5.5 to discuss quantitative improvements.

$$M_i = C\left(\frac{d}{2}\right) \tag{5.3}$$

$$C = T = E_s \varepsilon_s a_s \tag{5.4}$$

where, M_i: internal moment, C: passive compression on wall cross-section, T: restraint by rods, d: wall depth, E_s: Young's modulus of rods, ε_s: strain measured on rods, a_s: total cross-sectional area of rods.

The external moments of the strengthened specimens are higher than the internal resistances after cracking, while Eq. 5.3 evaluates the maximum resistances due to the maximum lever arm length with a half wall depth. These overevaluations of external moments seem to be caused due to losing uniform distribution loads given by the out-of-plane loading system. Lower normal stress might be partially applied around the middle span where a flexural crack formed a sharp bend hence a small gap between the specimen and airbag, as shown in Photos 5.5(b) and (c). Although the appropriate action of uniformly distributed loads had been verified for the loading system using an elastic plate in Chapter 4, the rubber airbag could not completely adapt the v-shaped deformation observed in the strengthened specimens. Therefore, it is concluded that the external moments of the strengthened specimens evaluated by Eq. 5.2 are not exactly reliable, and that analytical discussion should be done to quantitatively compare the maximum strengths between the control and strengthened specimens, as described in the next chapter.
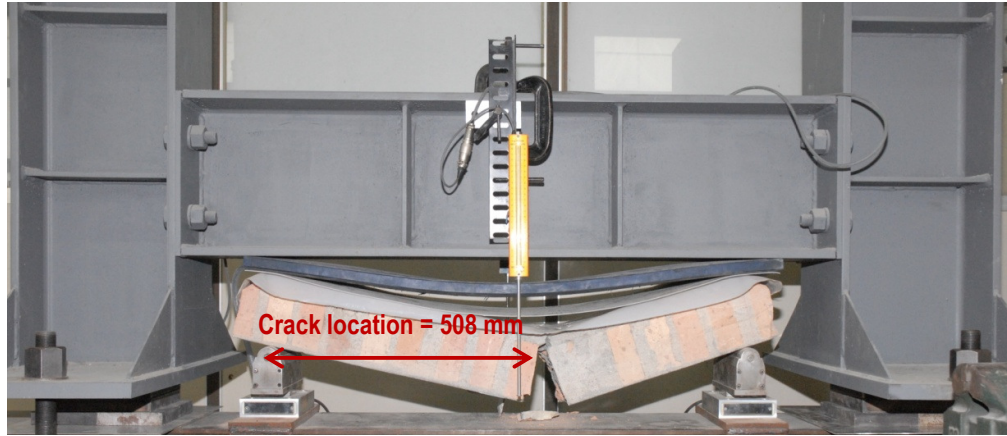
(a) ND after test
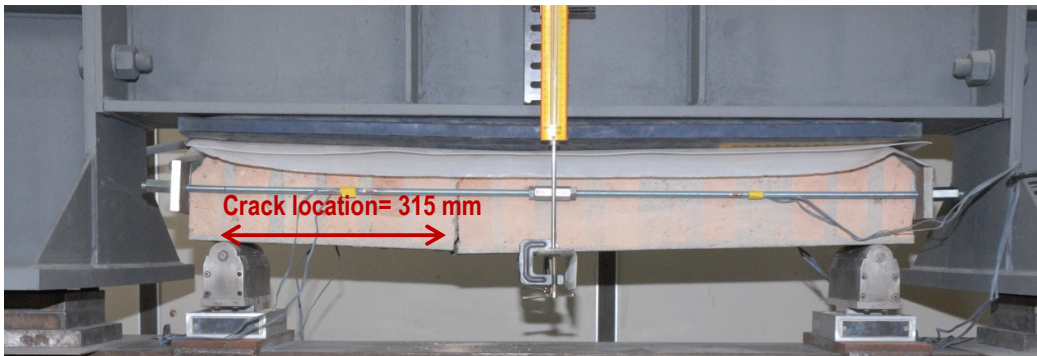
(b) SD at a 2.7% drift ratio
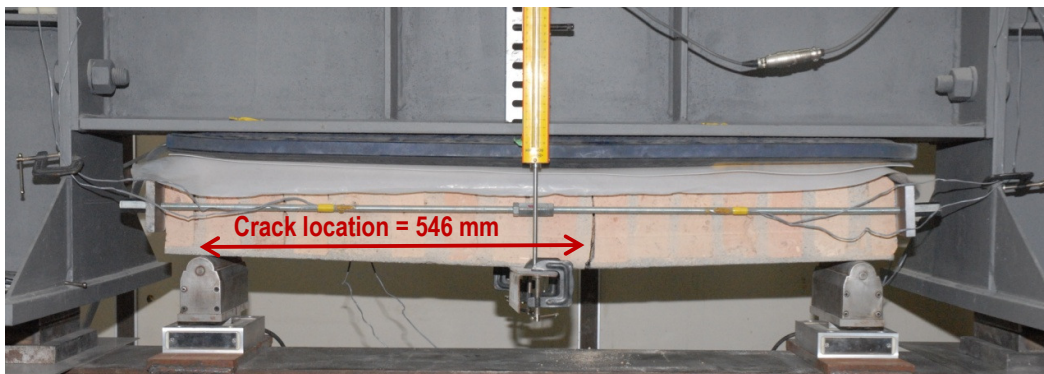
(c) SDI at 3.0% drift ratio

Photo 5.5 Damage to specimens after/during loading
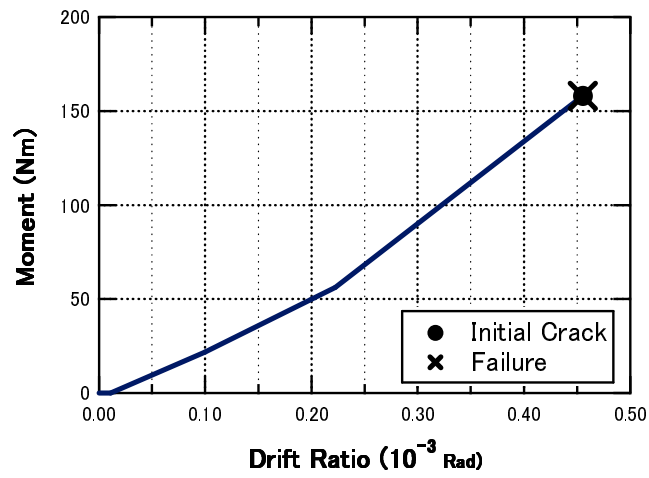
(a) N specimen
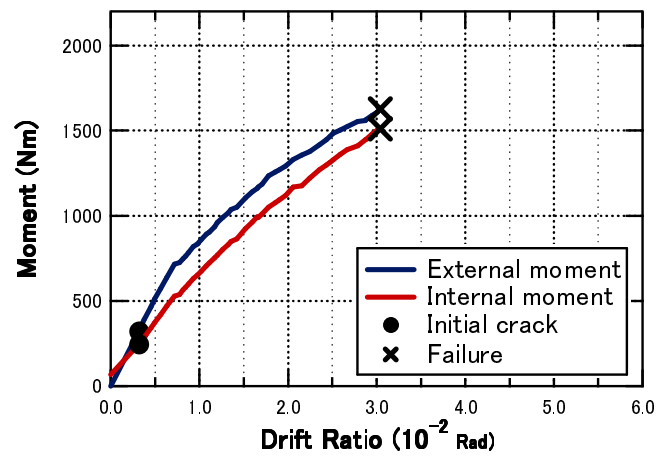
(b) S specimen
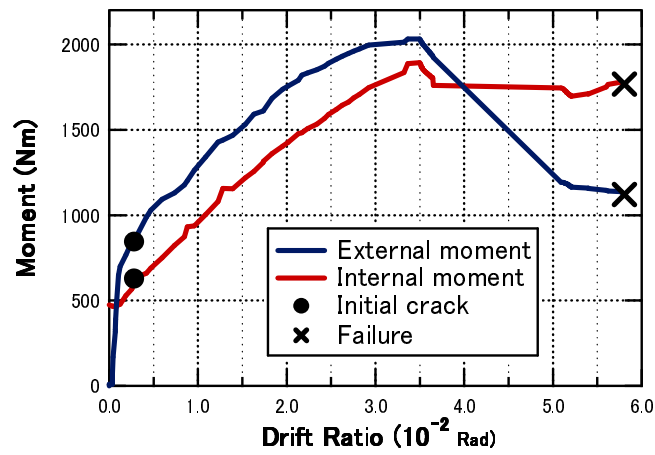
(c) SI specimen

Figure 5.5 Moment-drift angle relationships of specimens
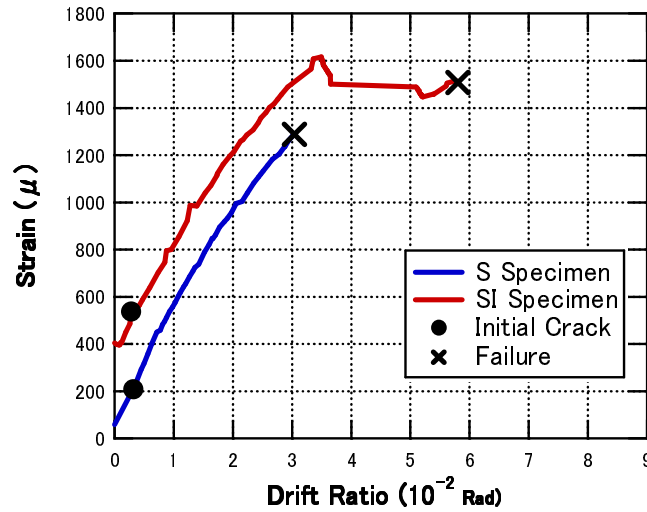
Figure 5.6 Strain-drift angle relationships of strengthened specimens

Figure 5.6 gives the averaged strain from gauges pasted on the rods of the strengthened specimens versus drift angle relationships. Tensile strain of each specimen increased according to an increase of drift angle, which means that a higher compression acted on the cross-section under a larger drift angle. As a result, the higher resistances could be obtained from the strengthened specimens under compression passively induced by the proposed strengthening system.

5.5   Summary

A new strengthening method, which utilized geometric deformation characteristics of masonry itself as well as restraint by steel rods, was proposed and verified to enhance the out-of-plane performance of masonry walls. The following conclusions were obtained from experimental studies.

6. Mechanism of the proposed strengthening was introduced. Out-of-plane performance

of masonry walls are enhanced by passive compression applied to wall cross-sections, which is caused by restraint of axial elongation of walls with their out-of-plane deformation.

7. The test results indicated that both of the strengrthened specimens exhibited much higher strengths and deformation capacities even after cracking of walls, nevertheless the unstrengthened specimen brittlely failed with the initial cracking. The proposed system can effectively improve the out-of-plane performance of masonry walls.

8. It was experimentally verified that the proposed strengthening mechanism provided the out-of-plane resistances under higher compression which acted on the wall cross section with increasing of tensile strains of strengthening rods.

5.6   References

Ismail N, Laursen P and Ingham JM (2009) "Out-of-Plane Testing of Seismically Retrofitted URM Walls Using Posttensioning", *Australian Earthquake Engineering Society (AEES) 2009 Conference*.

Maidiawati and Sanada Y. (2008) "Investigation and Analysis of Buildings Damaged during the September 2007 Sumatra, Indonesia Earthquakes", *Journal of Asian Architecture and Building Engineering*, 7(2):371–378.

Chapter 6

Analytical Evaluation of Out-of-plane Performance of Strengthened Masonry Walls

6.1   Introduction

The external moments of the strengthened specimens are higher than the internal resistances after cracking, while Eq. 5.3 evaluates the maximum resistances due to the maximum lever arm length with a half wall depth, which is described in Chapter 5. These overevaluations of external moments seem to be caused due to losing uniform distribution loads in the newly developed loading system. Lower normal stress might be partially applied around the middle span where a flexural crack formed a sharp bend hence a small gap between the specimen and airbag, as shown in Photos 5.5(b) and (c). Although the appropriate action of uniformly distributed loads had been verified for the loading system using an elastic plate in Chapter 4, the rubber airbag could not completely adapt the v-shaped deformation observed in the strengthened specimens.

Therefore, it is concluded that the external moments of S and SI specimens experimentally obtained are unreliable, and that analytical discussion should be done to quantitatively evaluate in terms of the internal moments only for S and SI.

The major objectives of this study are to present a theoretical calculation procedure to evaluate the out-of-plane performance of strengthened walls and to verify it comparing with the experimental test results.

6.2   Theoretical Performance Evaluation

It was experimentally found that a flexural crack opened close to the middle span of the strengthened specimens. Therefore, the experimental behavior is simplified to theoretically evaluate the performance of strengthened specimens, as shown in Figure 6.1. This analytical model assumes a rigid body for each wall separated by a flexural crack at the middle span, a symmetric rotation at a hinge at the middle span and the hinge depth of x_n which is equivalent to the depth of compression zone evaluated by Eq. 6.1. However, the stress block concept by American Concrete Institute (2011) is applied to the equation, as shown in Figure 6.2.

$$x_n = \frac{C}{0.85 \cdot b \cdot 0.85 \, f_m} \tag{6.1}$$

where, x_n: depth of compression zone, b: wall width, f_m: compressive strength of wall. A total axial elongation of wall is defined as an incremental length between the middle depths at both ends. Equation 6.2 gives an axial elongation of each separated wall with half length, Δ_e, as shown in Figure 6.1b. A geometric elongation due to rigid body

rotation of wall, Δ_g is caused by a rigid body rotation of R ($= \frac{\delta}{l/2}$, where δ : vertical deformation at the middle span, l: span length of wall). In the equation, however, shortenings of wall due to the geometric nonlinearity, Δ_n and the compressive deformation, Δ_c are considered. Consequently, an axial strain of restraint rods, ε_s is given by Eq. 6.3, and hence a restraining tension of T is obtained by Eq. 5.4. Conversely, a passive compression of C is applied to the wall as a reaction of T. A compressive deformation of wall, Δ_c, is calculated by Eq. 6.4.

.

Load

(a) Simplified behavior under loading

$\Delta g_1 = d/2 \sin R$

$\Delta g_2 = xn \sin R$

Detail①

Detail②

Geometric elongation

$\Delta n = \ell/2(1-\cos R)$

Detail③

Geometric nonlinear shortening

Compressive deformation

$\Delta e = \Delta g_1 - \Delta g_2 - \Delta n - \Delta c$

Total elongation

(b) Cumulative axial deformation of separated
wall with half length
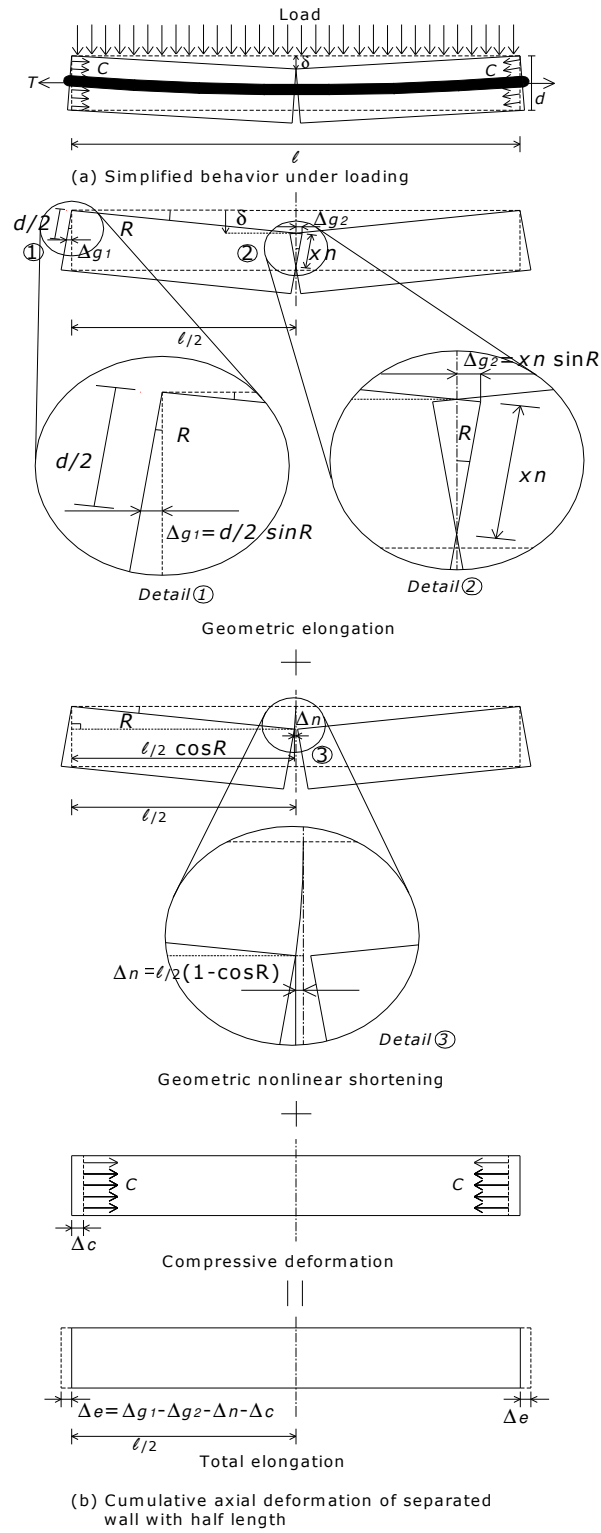
Figure 6.1 Analytical model for performance evaluation (symmetric model)
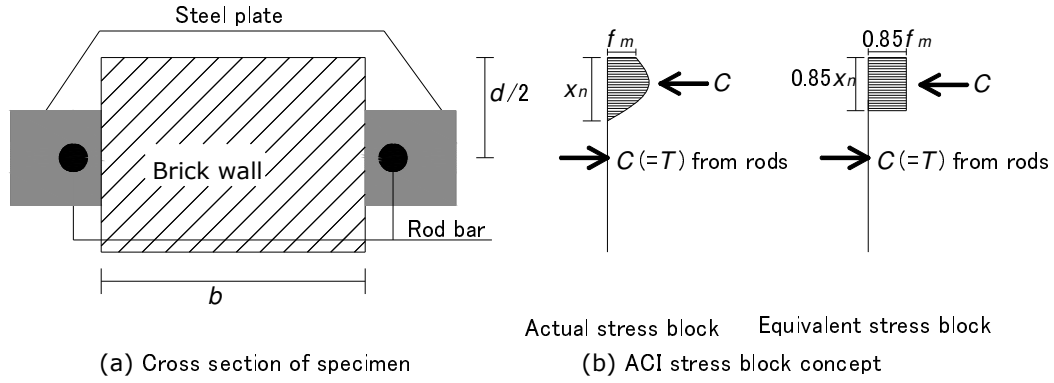
Figure 6.2 Stress distribution assumption

$$\Delta_e = \Delta_g - \Delta_n - \Delta_c = \left(\frac{d}{2} - x_n\right) sinR - \frac{l}{2}(1 - cosR) - \Delta_c \qquad (6.2)$$

$$\varepsilon_s = \frac{2\Delta_e}{l} = \frac{2(\Delta_g - \Delta_n - \Delta_c)}{l}$$

$$= \frac{(d - 2x_n)sinR}{l} - 1 + cosR - \frac{2\Delta_c}{l} \qquad (6.3)$$

$$\Delta_c = \varepsilon_m \frac{l}{2} = \frac{C}{E_m a_m} \frac{l}{2} \qquad (6.4)$$

where, ε_m : strain of masonry, E_m: Young's modulus of wall, a_m: averaged cross-sectional area of wall which defined by $b \cdot \frac{x_n + d}{2}$ based on an assumption of compression area as described in Figure 6.3. This assumption briefly represented a reduction of compression area at the crack, however, the interpolated reductions between the crack and wall ends had not been experimentally verified in this study.

(a) Cross section of specimen   (b) Compression area in half wall
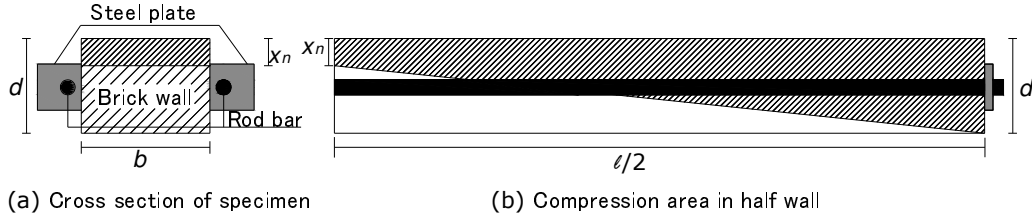
Figure 6.3 Assumption of compression area of wall

Observing the cracking behavior of strengthened specimens more precisely, they exhibited asymmetric behavior because a flexural crack occurred a little away from the middle span, as shown in Photo 5.3. Furthermore, the simplified model is modified to consider the location of crack, as shown in Figure 6.4.

The basic concept of asymmetric model is the same as that of symmetric model. The modified model gives a larger rotation angle of R' for the shorter separated wall, and different elongations of Δ_e' and Δ_e'' for the shorter and longer walls, which are represented by Eqs. 6.5 and 6.6, respectively. These results in a modified axial strain of restraint rods, ε_s', as shown in Eq. 6.7, which replaces Eq. 6.3 in the symmetric model.

$$R' = \frac{\delta'}{\frac{l}{2} - l_c} = \frac{\delta\left(1 + \frac{l_c}{\frac{l}{2}}\right)}{\frac{l}{2} - l_c} = \frac{\left(\frac{l}{2} + l_c\right)}{\frac{l}{2} - l_c} R \tag{6.5}$$

In case of the shorter side:

$$\Delta_e' = \left(\frac{d}{2} - x_n\right) sinR' - \left(\frac{l}{2} - l_c\right)(1 - cosR') - \Delta_c' \tag{6.6a}$$

In case of the longer side:

$$\Delta_e'' = \left(\frac{d}{2} - x_n\right) sinR - \left(\frac{l}{2} + l_c\right)(1 - cosR) - \Delta_c'' \qquad (6.6b)$$

$$\varepsilon_s' = \frac{\Delta_e' + \Delta_e''}{l} = \frac{\left[\left(\frac{d}{2} - x_n\right) sinR + \left(\frac{d}{2} - x_n\right) sinR'\right]}{l}$$

$$- \frac{\left[\left(\frac{l}{2} + l_c\right)(1 - cosR) + \left(\frac{l}{2} - l_c\right)(1 - cosR')\right] - 2\Delta_c}{l} \qquad (6.7)$$

where δ': vertical deformation at the crack location, l_c: length from the middle span to crack location, Δ_c', Δ_c'': compressive deformation of shorter and longer walls, however, $\Delta_c' + \Delta_c'' = 2\Delta_c$.

Load

T C δ' C T

d

$\ell/2$ ℓ_c $\ell/2 - \ell_c$

(a) Simplified behavior under loading

Crack location

$d/2$ R δ Δ_{g2}' δ' R' $d/2$

Δ_{g1} xn Δ_{g2} ① Δ_{g1}'

②

$\ell/2$ ℓ_c $\ell/2 - \ell_c$

$\Delta_{g2}' = xn \sin R'$

R'

xn

R'

$d/2$

$\Delta_{g1}' = d/2 \sin R'$

Detail①   Detail②

Geometric elongation

＋

③

R Δn R'

$(\ell/2+\ell_c)\cos R$ Δn $(\ell/2-\ell_c)\cos R'$

$\ell/2$ ℓ_c $\ell/2 - \ell_c$

$\Delta n' = (\ell/2-\ell_c)(1-\cos R')$

$\Delta n'' = (\ell/2+\ell_c)(1-\cos R)$

Detail③

Geometric nonlinear shortening

＋

C C

$\Delta c''$ $\Delta c'$

Compressive deformation

‖

$\Delta e'' = \Delta_{g1} - \Delta_{g2} - \Delta n'' - \Delta c''$ $\Delta e' = \Delta_{g1}' - \Delta_{g2}' - \Delta n' - \Delta c'$

$\ell/2$

Total elongation

(b) Cumulative axial deformation of wall
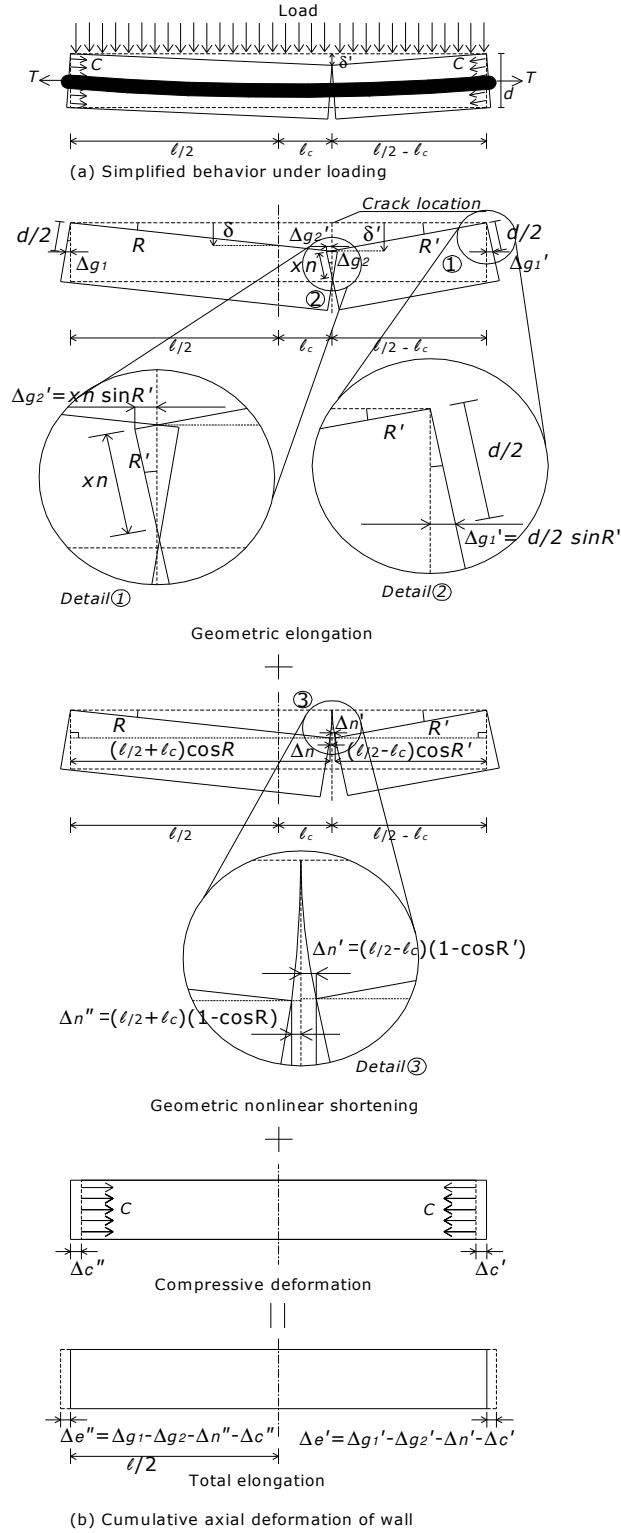
Figure 6.4 Analytical model for performance evaluation (asymmetric model considering crack location)

It should be noted that an iterative process is needed to obtain the total restraint by rods and the passive compression on wall cross-section. It is carried out according to a flowchart in Figure 6.5.


```
                        ┌──────────────┐
                        │    START     │
                        └──────────────┘
                               │
                               ▼
                        ┌──────────────┐
                        │   Give R     │
                        └──────────────┘
                               │
                               ▼
                   ┌──────────────────────┐
                   │ Assume initial value │
                   │      of C_0          │
                   └──────────────────────┘
                               │
                               ▼
                   ┌──────────────────────┐
                   │ Calculate x_n by     │◄──────────┐
                   │ Eq. 6.1              │           │
                   └──────────────────────┘           │
                               │                       │
                               ▼                       │
              ┌─────────────────────────────────┐      │
              │ Calculate ε_s by Eqs. 6.2 and    │      │
              │ 6.3 or Eqs. 6.6 to Eq. 6.7       │      │
              └─────────────────────────────────┘      │
                               │                       │
                               ▼                       │
              ┌─────────────────────────────────┐      │
              │ Obtain T or C by Eq. 5.3        │      │
              └─────────────────────────────────┘      │
                               │                       │
                               ▼             No  ┌──────────────┐
                          ◇ C = C_0 ? ──────────►│  C = C_0     │
                               │                 └──────────────┘
                              Yes
                               ▼
                        ┌──────────────┐
                        │   FINISH     │
                        └──────────────┘
```
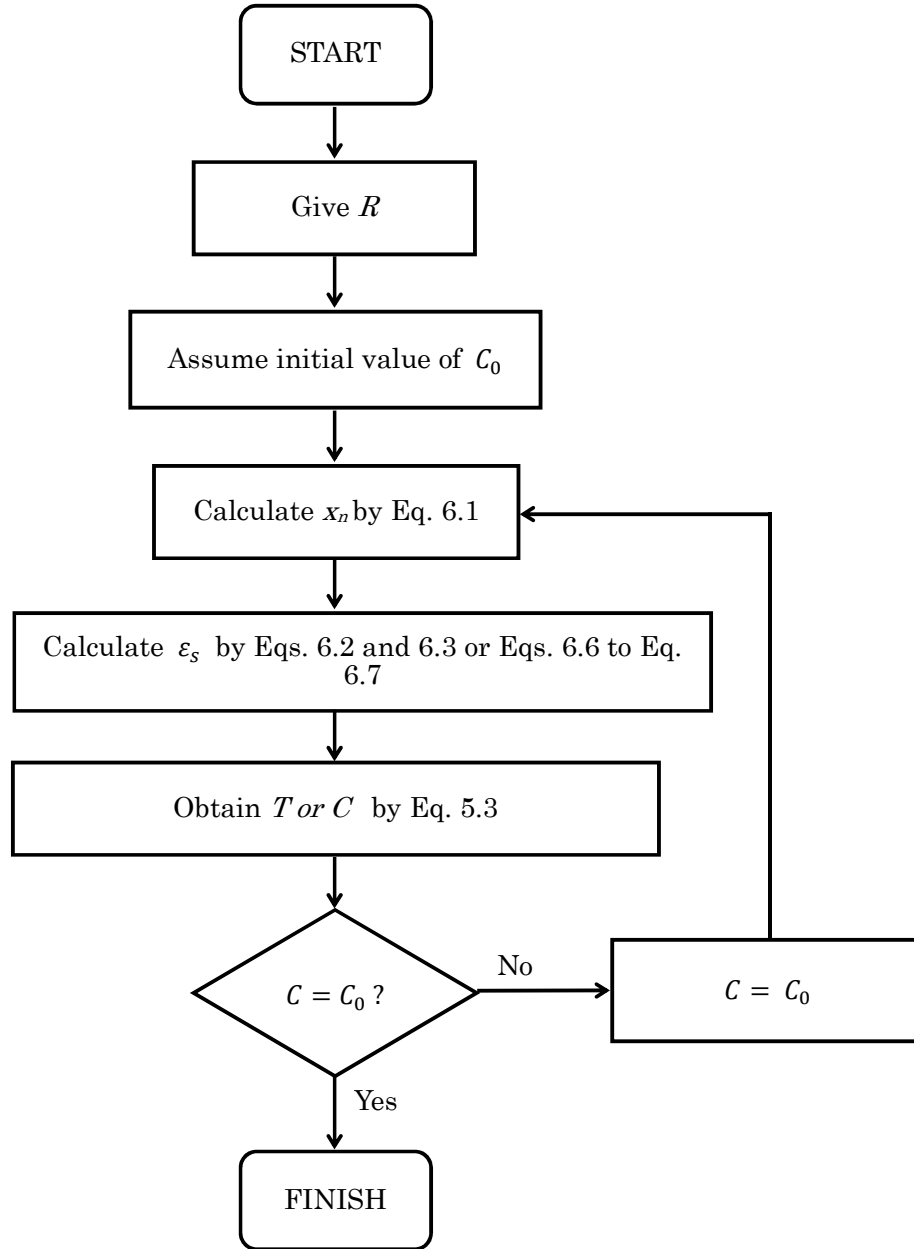
Figure 6.5 Flowchart for identifying passive compression

6.3   Performance Curves of Strengthened Masonry Walls

As described in Chapter 5, the external moments of the strengthened specimens are higher than the internal resistances, therefore the analytical discussion should be conducted on the internal moments only for S and SI. Figure 6.6 gives the relationships between internal moment and drift angle for strengthened specimens.

Figure 6.7 gives the averaged strain from gauges pasted on the rods of the strengthened specimens versus drift angle relationships. Tensile strain of each specimen increased according to an increase of drift angle, which means that a higher compression acted on the cross-section under a larger drift angle. As a result, the higher resistances could be obtained from the strengthened specimens under compression passively induced by the proposed strengthening system.
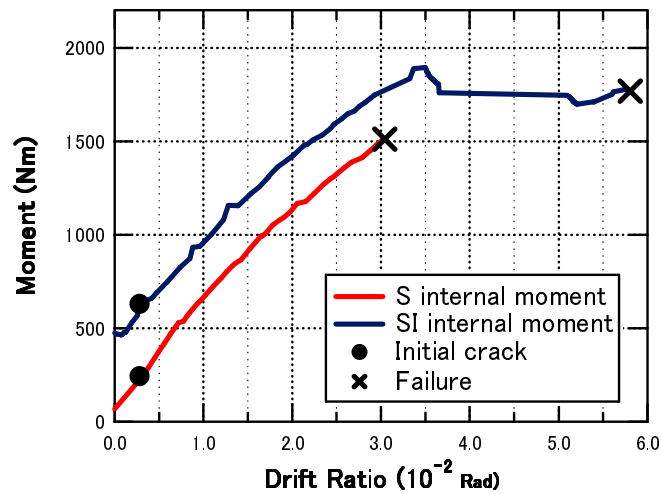
Figure 6.6 Moment-drift angle relationships of strengthened specimens
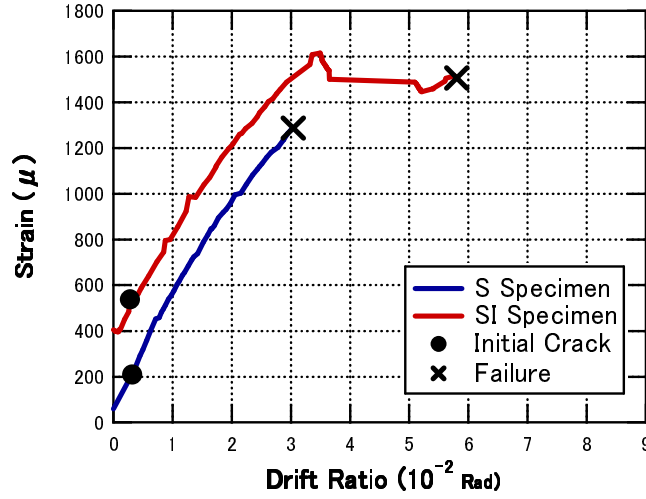
Figure 6.7 Strain-drift angle relationships of strengthened specimens

6.4　Performance Comparisons with Experiment Results

The relationships between strain of rods and drift angle are obtained for the strengthened specimens through determining *C* (or *T*) by the iterative process and compared to the experimental results in Figure 6.8. The performance curves, namely the moment vs. drift angle relationships of the strengthened specimens are also obtained and compared with the experimental results in Figure 6.9. In this figure, however, the moment means an internal moment evaluated by Eq. 6.8 based on a distance of compression couple, as shown in Figure 6.2. The experimental internal moments are also obtained in the same manner based on the measured rod strains by Eq. 5.3, because of unreliable external moments mentioned in the previous chapter.

$$M_i' = C \ or \ T \ \cdot \left(\frac{d}{2} - \frac{o.85 \ x_n}{2} \right) \tag{6.8}$$

Good agreements are obtained for both relationships in these figures 6.8 and 6.9,

which verifies the performance evaluation method presented above. However, a little higher deformation capacities are evaluated by the theoretical evaluations, which seems to be caused by the stress block assumption adopted as shown in Figure 6.2.

Consequently, it is found from the experimental relationships in Figure 6.9 that the maximum strengths of about 1000 kNm exceeded more than 6 times compared to that of the control specimen (refer to Figure 5.5a) by the proposed strengthening method. Moreover, the initial strain applied to the SI specimen did not effectively contribute to the maximum strength, while a larger deformation/crack opening was observed under a lower moment for the S specimen. These results verify the rational strengthening mechanism of the proposed method, because cracks are likely to close not only under pre-tension but also under passive compression after unloading.
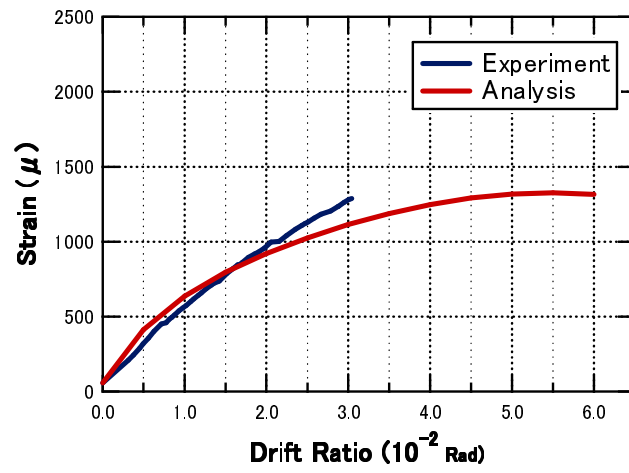
(a) S specimen
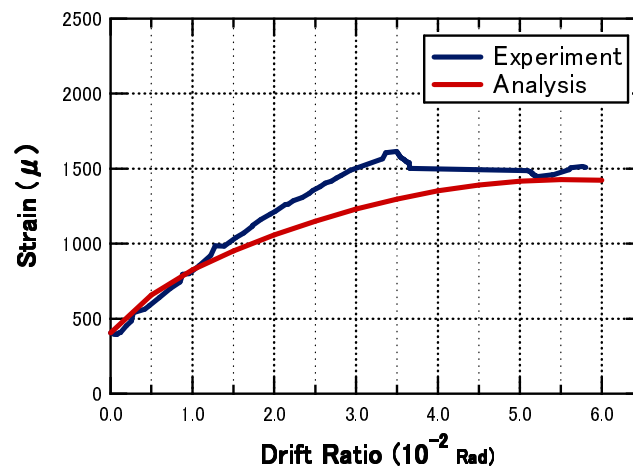
(b) SI specimen

Figure 6.8 Comparisons of strain vs. drift angle relationships between tests and
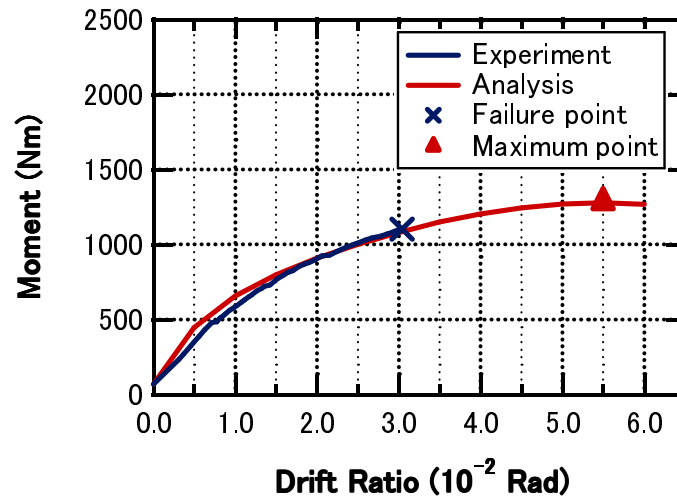
analyses

(a) S specimen
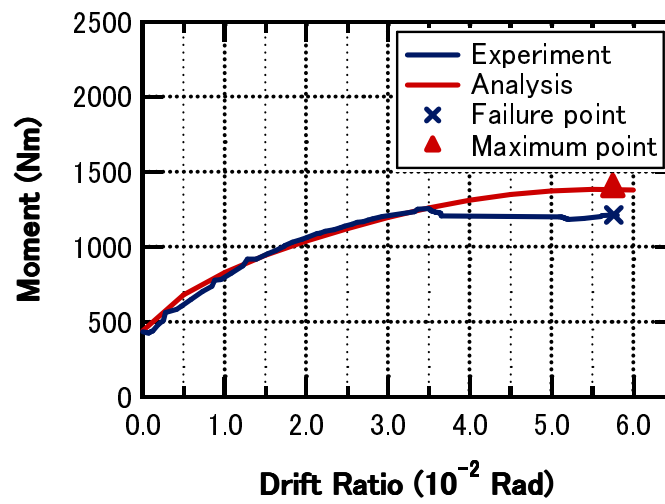
(b) SI specimen

Figure 6.9 Comparisons of moment vs. drift angle relationships between tests and

analyses

6.5   Application of Proposed Strengthening to Typical Cantilever Walls in Aceh

The proposed strengthening system and analytical method were implemented to typical cantilever walls in Aceh. The calculation for out-of-plane performance evaluation was conducted by assuming several ratios of rebar sectional area and wall depths. The typical brick masonry walls which are used in Aceh have the dimensions and weight described in Chapter 3.5 and shown in Figure 3.9.

Figure 6.10 shows effects of the weight of wall itself on the out-of-plane performance, where W: typical weight of wall (250 kg/m^2 in the case of wall depth of d and 450 kg/m^2 for wall depth of $2d$) and $R = \frac{\delta}{l}$.
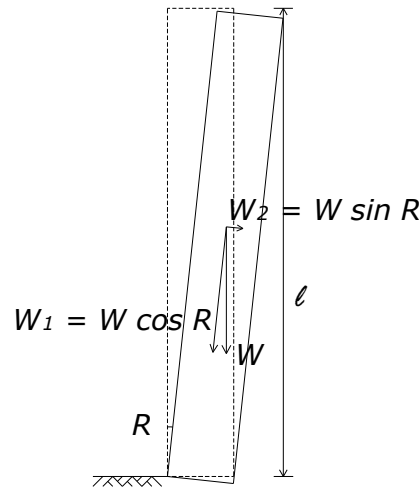
Figure 6.10 Effects of wall weight on out-of-plane performance

By using the concept of theoretical performance evaluation above, a total axial elongation of wall is defined as an incremental length at the bottom end, as shown in Figure 6.11. Equation 6.9 gives an axial elongation, Δ_e, as shown in Figure 6.11b. A geometric elongation due to rigid body rotation of wall, Δ_g is caused by a rigid body

rotation of R ($= \frac{\delta}{l}$, where δ : vertical deformation, l: span length of wall). However, shortenings of wall due to the geometric nonlinearity, Δ_n and the compressive deformation, Δ_c are considered in the equation. Consequently, an axial strain of restraint rods, ε_s is given by Eq. 6.10, and hence a restraining tension of T is obtained by Eq. 5.4. Conversely, a passive compression of C is applied.

(a) Simplified behavior under loading

(b) Cumulative axial deformation of wall

Geometric elongation

Geometric shortening

Geometric nonlinear shortening

Compressive deformation

Total elongation

(b) Cumulative axial deformation of wall
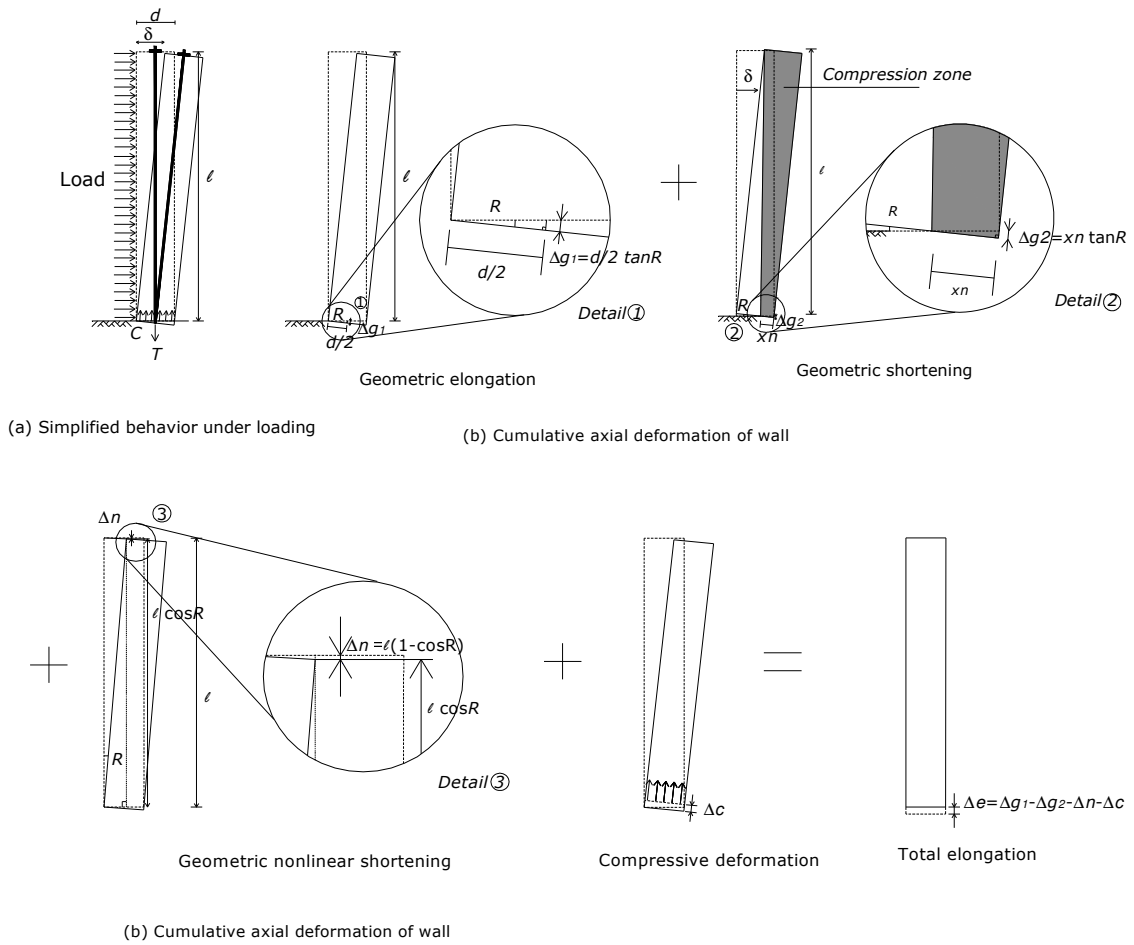
Figure 6.11 Deformation image of cantilever wall

$$\Delta_e = \Delta_g - \Delta_n - \Delta_c = \left(\frac{d}{2} - x_n\right) tanR - l\,(1 - cosR) - \varepsilon_m\,l \qquad (6.9)$$

$$\varepsilon_s = \frac{\Delta_e}{l} = \frac{\left(\Delta_g - \Delta_n - \Delta_c\right)}{l} = \frac{\left(\frac{d}{2} - x_n\right) tanR}{l} - 1 + cosR - \frac{\Delta_c}{l} \qquad (6.10)$$

$$\Delta_c = \varepsilon_m\,l \;\; = \frac{C}{E_m a_m}\,l \qquad (6.11)$$

$$\text{and} \qquad a_m \;=\; \frac{x_n + d}{2}\,b \qquad (6.12)$$

Considering the wall weight as show in Figure 6.10, the moment capacity becomes:

$$M_i^{''} = (C\ or\ T + W_1) \cdot \left(\frac{d}{2} - \frac{0.85\,x_n}{2}\right) \qquad (6.13)$$

and,

$$W_1 = W\cos R \qquad (6.14)$$

where x_n: depth of compression zone, b: wall width, f_m: compressive strength of wall, d: wall depth, Δ_g: a geometric elongation due to rigid body rotation of wall which caused by a rigid body rotation of R where, $R = \frac{\delta}{l}$, Δ_n : shortening of wall due to the geometric nonlinearity, Δ_c.: the compressive deformation, ε_s: an axial strain of restraint rods, T : restraining tension, C: passive compression applied to the wall as a reaction of T. $M_i^{''}$: moment capacity, W_1 : axial stress on wall section due to weight, as show in Figure 6.10, W: weight of wall.

This calculation also assumes rebar ratio to wall sectional area P_t and wall depth of d:

$$P_t = \frac{Rebar\ area}{wall\ area} = \frac{n\,a_s}{b\,d} \qquad (6.15)$$

where *n*: number of rebars, a_s: area of rebar (= 36.6 mm^2). The following calculations assume P_t of0.1%, 0.2%, 0.3%, 0.4%, and 0.5%, and wall depths of *d* and *2d*.

Figure 6.12 shows the relationship of moment capacity of wall and drift ratio at several P_t ratios and wall depth of d. Under these conditions, the calculation cannot be completed in the case s of P_t of 0.3% to 0.5%. This was due to greater x_n than half of wall depth. Figure 3 shows the relationship of moment capacity of wall and drift ratio with different P_t ratios and wall depth of 2d. In this case, the calculation cannot be completed for P_t of 0.5% because of the same reason. Both of these figures show that the proposed strengthening method can be applied to typical masonry walls and generate much higher strengths than un-strengthened wall.
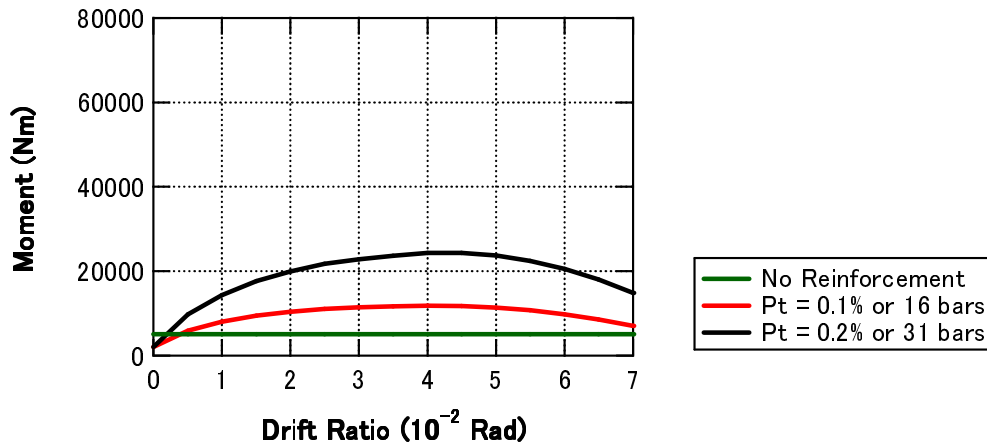
Figure 6.12 Moment capacity at the bottom for *1d* depth wall
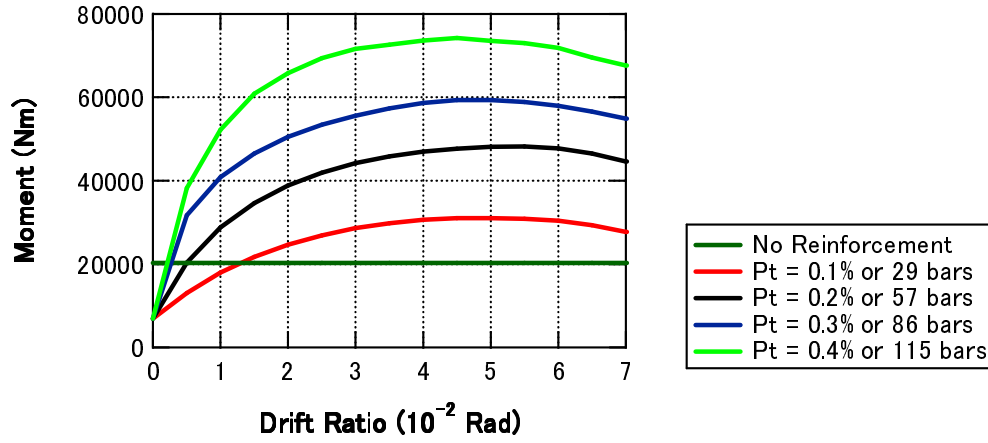
Figure 6.13 Moment capacity at the bottom for *2d* depth wall

At the maximum moment of each P_t ratio, the load carrying capacity of wall *F* can be obtained by:

$$M = \frac{w\ l^2}{2} \qquad and \qquad F = w\ \cdot l \qquad\qquad (6.16)$$

So,

$$F = w\ l = \frac{2\ M}{l^2}\ .l \qquad\qquad (6.17)$$

The equivalent acceleration *A* is:

$$A = \frac{F}{W}\ G \qquad\qquad (6.18)$$

where *w*: distribution load, *l*: height of wall, *F*: load carrying capacity of wall, *G*: gravity acceleration = 9.8 m/s^2 and *A* : equivalent acceleration.

Table 6.1 shows the load carrying capacities for all analytical cases. The results show that the wall might fail under an acceleration of 0.27 G to 0.94 G. Based on the

information on shakemap of Figure 3.1, the maximum intensity estimated by USGS (2013) for the site was about 0.24 G, which means that masonry walls would withstand the 2013 event by the strengthning method proposed in this study.

Table 6.1   Calculation results

Depth wall	P_t (%)	Number of rebars	Mmax (Nm)	Acceleration (G)
d	0.1	16	11817.99	0.27
	0.2	31	24328.94	0.55
2d	0.1	29	31078.08	0.39
	0.2	57	48240.52	0.61
	0.3	86	59384.73	0.75
	0.4	115	74665.35	0.94

6.6   Summary

9. A theoretical calculation procedure is presented for the out-of-plane performance evaluation of masonry walls strengthened by the proposed method.

10.   The performance curves of the strengthened specimens showed good agreements between the experiments and analyses, which means that the presented calculation procedure can evaluate the out-of-plane performance of strengthened specimens well.

11.   Due to the technical problem of the out-of-plane loading system, however, the experimental performance was represented by the internal moment, which was obtained by estimating the neutral axis depth at the location of crack. Consequently, it was found that the maximum strengths were improved by about 6 times by the

proposed strengthening method.

12. The initial strain applied to the rods contributed to reduce the out-of-plane deformation but did not affect the maximum strength. These results verify the proposed method without post-tensioning can effectively prevent out-of-plane failure of masonry walls.

13. The performance of typical masonry walls in Aceh was re-evaluated by applying the proposed analytical method. Consequently, the proposed system could effectively improve the out-of-plane performance of masonry walls.

6.7 References

American Concrete Institute (ACI) (2011) "Building Code Requirements for Structural Concrete (ACI 318-11) and Commentary".

USGS website: http://www.usgs.gov/

Chapter 7

Summary and Conclusions

7.1   Summary

Masonry is one of the oldest structural systems and commonly used in building construction throughout the world. Masonry walls typically have low flexural capacities and possess brittle failure modes when exposed to out-of-plane loads. Many experimental studies have been conducted by a number of researchers to investigate the out-of-plane behavior of masonry structures. As the results, they pointed out its vulnerability and importance of strengthening. Therefore, in the seismic area such as Indonesia, the strengthening of masonry walls must be considered to reduce future earthquake disasters.

This study was prefaced by the author's investigation on damaged buildings by the 2013 Aceh, Indonesia earthquake. Detailed investigation was carried out to investigate the out-of-plan performance of masonry walls in the affected area. As a

result, it was found that the severe damage to confined masonry structures was mainly caused by out-of-plane loads.

Experimental out-of-plane performance evaluation of masonry walls is essential to accomplish this study. Therefore, a new out-of-plane loading system was developed to investigate the out-of-plane performance of masonry walls under uniform distributed loads. The test system was developed aiming at obtaining basic mechanical characteristics of simply supported masonry walls in the out-of-plane direction.

New out-of-plane strengthening method was proposed to upgrade the out-of-plane performance of masonry walls. It utilized geometric deformation characteristics of masonry itself as well as restraint by steel rods. According to the test results on masonry walls with/without strengthening, the proposed system can effectively improve the out-of-plane performance of masonry walls.

Moreover, based on the test results, a new analytical model was proposed for estimating the out-of-plane performance of strengthened masonry walls. This model represented the specific behavior of strengthened walls from experimental results. Good agreements were obtained between analytical and experimental results, which verified that the proposed model could be used for estimating the out-of-plane performance of strengthened masonry walls.

7.2   Conclusions

As the results of the current study, the following conclusions have been reached;

1. According to field investigation conducted after the July 2013 Aceh, Indonesia earthquake in the affected area close to the epicenter of earthquake, it revealed that the confined masonry structures suffered from moderate to heavy damage/totally

collapse and that the major cause was out-of-plane failure of masonry walls.

2. A new out-of-plane loading system was developed by using a rubber airbag for evaluating structural performance of masonry walls in the out-of-plane direction and verified through comparing the experimental measurements and theoretical caluculations.

3. Mechanism of the proposed strengthening was introduced. The proposed system was verfied to effectively improve the out-of-plane performance of masonry walls through a series of structural tests using Indonesian typcial masonry walls with/without strengthened by it. Quantitative improvements by the strengthening were discuessed with the following analytical model also prenseted in this study.

4. A theoretical calculation procedure was presented for the out-of-plane performance evaluation of masonry walls strengthened by the proposed method. The performance curves of the strengthened specimens showed good agreements between the experiments and analyses, which means that the presented calculation procedure can evaluate the out-of-plane performance of strengthened specimens well.

5. Initial strain applied to the rods contributed to reduce the out-of-plane deformation but did not affect the maximum strength. These results verified that the proposed method without post-tensioning can effectively prevent out-of-plane failure of masonry walls.

6. Applying the proposed analytical method to typical masonry walls in Aceh, it was shown that the proposed strengthening method significantly contributed to upgrade the out-of-plane performance masonry walls.

7.3 Recommendations

According to the experimental and analytical results, the proposed strengthened method has a significant impact to increase the out-of-plane performance of masonry walls.

In current study, the effectiveness of proposed method was experimentally verified using small dimensions of specimens. In the future, therefore, the method is recommended additionally to be verified by applying it to real dimensions of walls, especially typical walls in Aceh.

On the other hand, the presented analytical model can be applied to evaluate the out-of-plane performance of masonry walls strengthened by the proposed method. In the future, this model can be implemented for practical design through establishing a technical guideline for strengthening system to prevent masonry walls from the out-of-plane failure.

References

American Concrete Institute (ACI) (2011) "Building Code Requirements for Structural Concrete (ACI 318-11) and Commentary".

Arya A.S., Boen T. and Ishiyama Y. (2013) "Guideline For Earthquake Resistant Non-engineered Construction", *United Nations Educational, Scientific and Cultural Organization (UNESCO).*

Augenti N., Nanni A. and Parisi F. (2013) "Construction Failure and Innovative Retrofitting", *Buildings 2013*, Vol. 3, pp. 100-121.

Bultot E, Van Parys L, Datoussaid S. (2012) "Out-of-plane Behaviour of URM Walls: Experimental studies", *9th National Congress on Theoretical and Applied Mechanics*, Brussels.

Bajpai K. and D. Duthinh (2003) "Bending Performance of Masonry Walls Strengthened with Near-surface Mounted FRP Bars", *9th North American Masonry Conference*.

D. Dizhur, H. Derakhsan, J.M. Ingham, M.C Griffith. (2009) "In-situ Out-of-plane Testing of Unreinforced Masonry Partition Walls", *11th Canadian Masonry Symposium*, Toronto, Ontario, May 31-June 3.

Elgwady Mohamed A., Pierino Letuzzi, And Marc Bodouc. (2002) "Dynamic In-Plane Behavior of URM Wall Upgraded with Composites", *Third International Conference on Composite in Infrastructure*, 2002

ElGawady M, Lestuzzi P and Badoux M (2004) "A Review of Conventional Seismic Retrofitting Techniques for URM", *13th International Brick and Block Masonry Conference.*

F. Mosele, F. Porto, C. Modena, A. Fusco, G. Cesare, G. Vasconcelos, V. Haach, P. Lourenco, I. Beer, U. Schmidt, W. Brameshuber, W. Scheufler, D. Schermer and K. Zirch (2006) "Developing Innovative Systems for Reinforced Masonry Walls", *Diswall project report*, Italy.

Griffith M.C and Vaculik J. (2007) "Out-of-plane Flexural Strength of Unreinforced Clay Brick Masonry Walls", *The Masonry Society Journal*, September, Vol 25, No. 1, pp. 53-68.

Grunthal G. (1998) "European Macroseismic Scale 1998", Conseil de L'Europe Cahiers du Centre Europeen de Geodynamique et de Seismologie, Luxembourg, 1998.

Hamoush S.A, M.W. McGinley, P. Mlakar, D. Scott and K. Murray (2001) "Out-of-plane Strengthening of Masonry Walls with Reinforced Composites", *Journal of Composites for Construction*, Vol. 5, No. 3, pp. 139-145.

Hendry E.A.W. (2001) "Masonry Walls: Material and Construction", *Construction and Building Material, Elsevier*, Vol. 15, pp. 323-330.

Hrynyk T.D and Myers J.J. (2008). "Out-of-Plane Behavior of URM Arching Walls with Modern Blast Retrofits: Experimental Results and Analytical Model", *Journal of Structural Engineering*, 1589-1597.

http://unicefindonesia.blogspot.jp/2013/07/after-earthquake-in-aceh-indonesia.html

Ismail N, Laursen P and Ingham JM (2009) "Out-of-Plane Testing of Seismically Retrofitted URM Walls Using Posttensioning", *Australian Earthquake Engineering Society (AEES) 2009 Conference*.

Maidiawati (2013) "Modeling of Brick Masonry Infill for Seismic Performance Evaluation of RC Frame Buildings", *PhD Thesis, Toyohashi University of Technology.*

Maidiawati and Sanada Y. (2008) "Investigation and Analysis of Buildings Damaged during the September 2007 Sumatra, Indonesia Earthquakes", *Journal of Asian Architecture and Building Engineering*, 7(2):371–378.

Mosalam K., Glascoe L., Bernier J. (2009) "Mechanical properties of unreinforced brick masonry." *section 1, LLNL-TR-*417646.

Mosalam K, and Hashemi A., (2007) "Seismic Evaluation of Reinforced Concrete Buildings Including Effects of Masonry Infill Walls", *Peer Report 2007/100*, Pacific Earthquake Engineering Research Center, University of California, Berkeley.

Paulopereira MF, Netopereira MF, Diasferreira JE and Lourenco PB (2011) "Behavior of Masonry Infill Panels in RC Frames Subjected to In Plane And Out Of Plane Loads", *7th International Conference AMCM*, Poland.

Takiyama N, T. Nagae, H. Maeda, M. Kitamura, N. Yoshida and Y. Araki (2008) "Cyclic Out-of-Plane Flexural Behavior of Masonry Walls Rehabilitated by Inserting Stainless Pins", *14th World Conference on Earthquake Engineering*.

USGS website: http://www.usgs.gov/

Swe Zin Win, Maidiawati and Yasushi Sanada. (2011) "Seismic Performance of Nonstructural Brick Walls Used in Indonesian R/C Buildings Part 3: Earthquake Response Analyses of a Damaged Building", *Summaries of Technical Papers of Annual Meeting Architectural Institute of Japan*, C-2, Structure IV, pp. 943-944.

Zhimmerman. T, and Strauss. A. (2012) "Masonry and Earthquakes: Material Properties, Experimental Testing and Design Approaches", *InTech, Europe*.

Appendix A

Experiment Results on Three-point Bending Tests for

Proposal of Strengthening Method for Masonry walls

A.1   Specimens and Measurements

The proposed strengthening method was applied to brick wall specimens which were extracted from an earthquake-damaged building in Indonesia. Two brick wall specimens were prepared with the dimensions of 190 mm x 140 mm x 900 mm in width x thickness x length (height), as shown in Photo 5.2 and Table A.1. Young's modulus and compressive strength in the longitudinal direction of the specimens are 1.93 kN/mm^2 and 2.91 N/mm^2, respectively, as shown in Table A.2.

Two specimens were strengthened by M8 steel rods which were placed along the wall length and fixed to steel end plates provided at the wall ends, as shown in Photo 5.3 and Figure 5.3. Although all the strengthened specimens had the common structural specifications as mentioned in chapter 5, they were tested under different loading and

initial conditions, as shown in Table A.1. SP and SPI specimens were subjected to three-point bending loads. However, initial tensile strains were applied only to the rods of SPI specimen to induce initial compression on the cross-sections. The cross-sectional area, Young's modulus, and yield strength of the rods are shown in Table 5.2, respectively.

Table A.1 Experimental parameters

Specimen	SP	SPI
Strengthening*	S	S
Loading method**	P	P
Initial strain***	0	500

* N: none, S: strengthened.
** P: three-point bending load.
*** Unit: μ

Table A.2 Material properties of specimens

Specimen	SP	SPI
Brick Wall		
Young's modulus (kN/mm^2)	1.93	1.93
Compressive strength (N/mm^2)	2.91	2.91
Steel Rods		
Cross-sectional area (mm^2)	36.6	36.6
Young's modulus (kN/mm^2)	201	201
Yield stress (N/mm^2)	479	479
Tensile strength (N/mm^2)	708	708
Initial strain*/stress** (μ / N/mm^2)	0/0	500/0.28

* tensile strain of rod.

** compressive stress on wall cross-section.

A.2   Experimental Methods

Photo A.1 shows a typical loading system for three-point bending tests on SP and SPI specimens. Details of the systems can be referred to Figure A.1. Set-up of measurements for loading tests can be seen in Figure A.2. Vertical deformations were measured at the middle span of the specimens. The figure also shows locations of strain gauges on the steel rods of the strengthened specimens, which were installed to measure tension of strengthening rods and compression acted on the wall cross-sections.
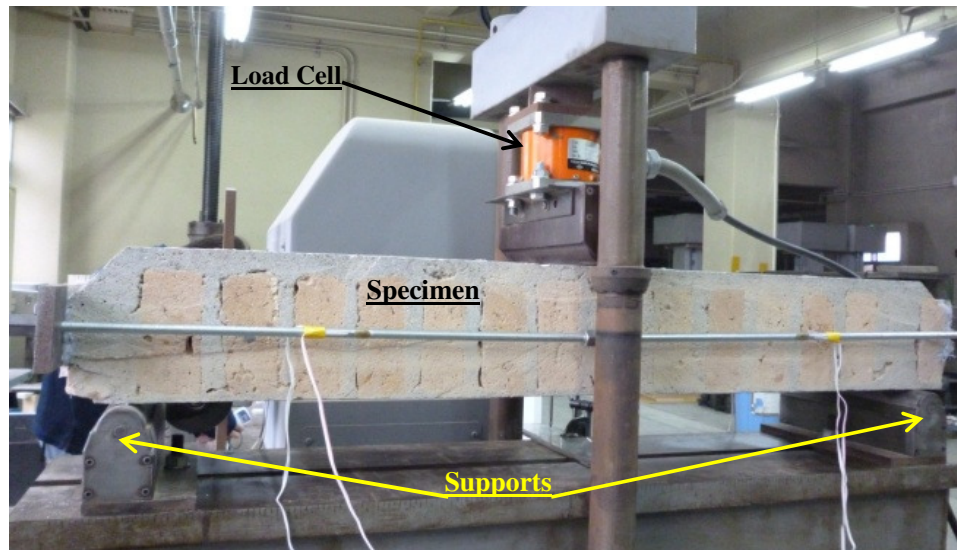
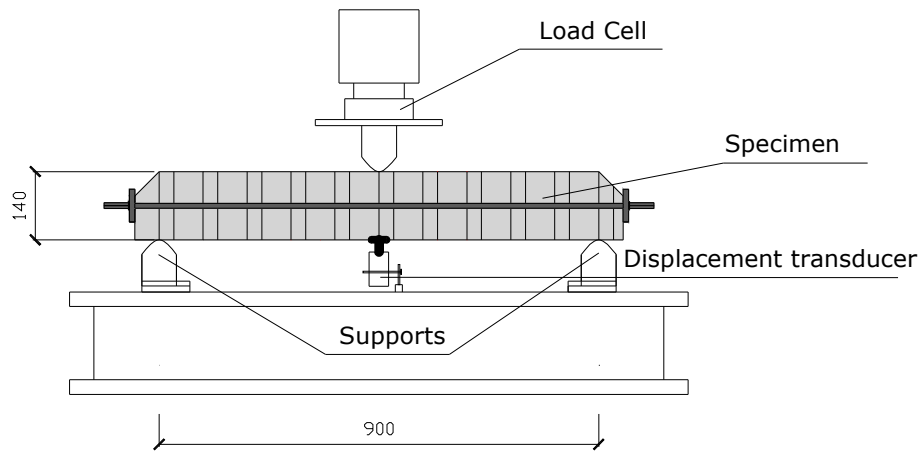Photo A.1 Front view of out-of-plane loading system for three-point bending test

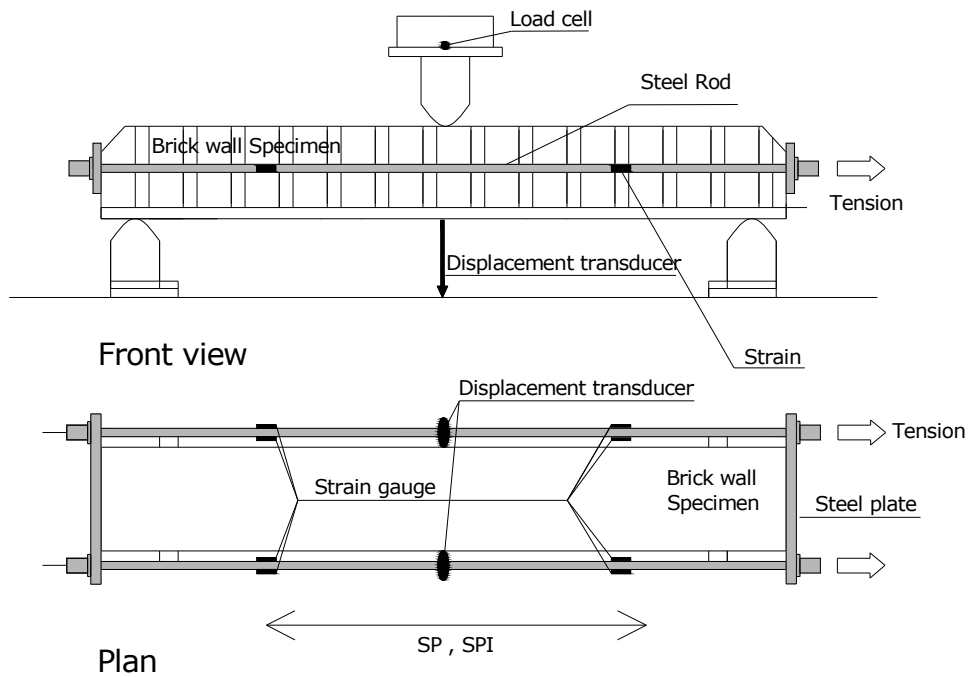Figure A.1 Details of out-of-plane loading system for three-point bending tests

Figure A.2 Test set-up for three-point bending tests

A.3   Experiment Results

Figure A.3 compares the relationships between external moment and drift angle at the middle span between the strengthened and unstrengthned specimens, respectively. However, the external moment was evaluated by Eq. A.1, and the drift angle was defined dividing the vertial deformation by half of the wall length.

$$M_e = \frac{Pl}{4} \tag{$A.1$}$$

where, M_e: external moment, P: total load, l: wall length.

It shows that the strengthened specimens exhibited much higher resistances even after cracking. Photo A.2 shows the specimens after cracking. It is found that the strengthened specimens sustained out-of-plane loads after a flexural crack occurred and opened. The drift angles at the maximum moments were around 3.0% rad. for SP specimen, however SPI in which unexpected slippage occurred between the steel end plate and specimen at 2.0% rad., as indicated in Figure. A.3(b).

Moreover, in the cases of strengthned specimens, the external moments are also compared to the internal resistances evaluated by Eq. 5.3 and Eq. 5.4 in Figure. A.3 to discuss quantitative improvements. This figure shows that the external moments and internal resistances of SP and SPI specimens approximately agreed after craking.
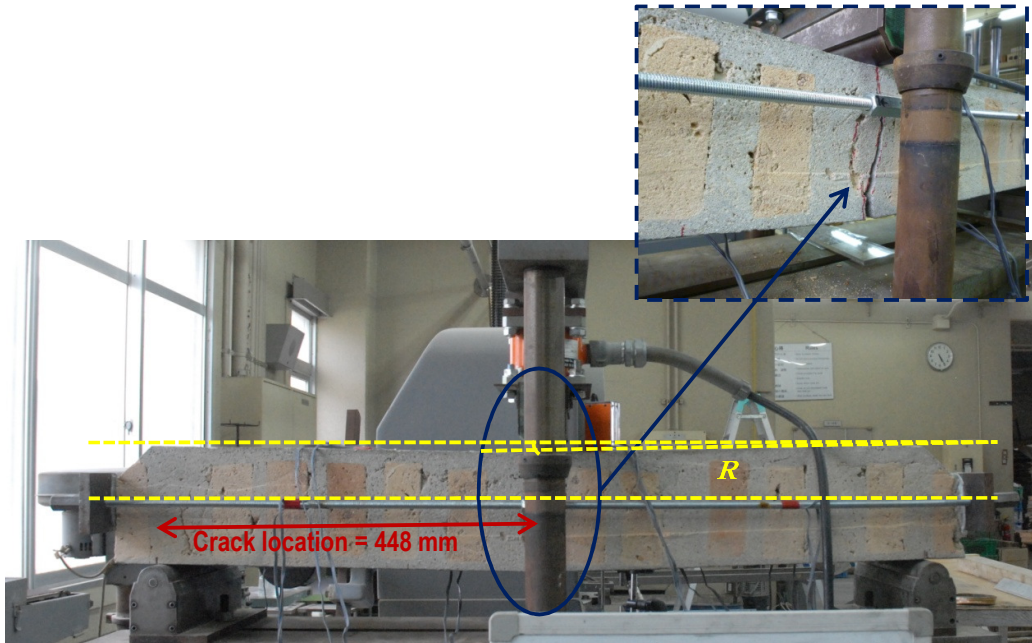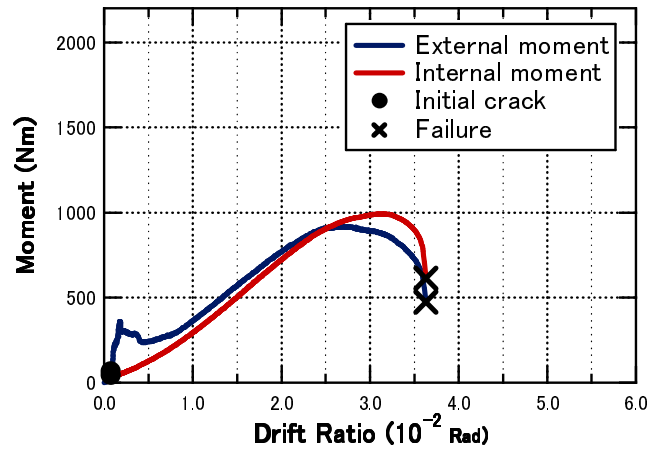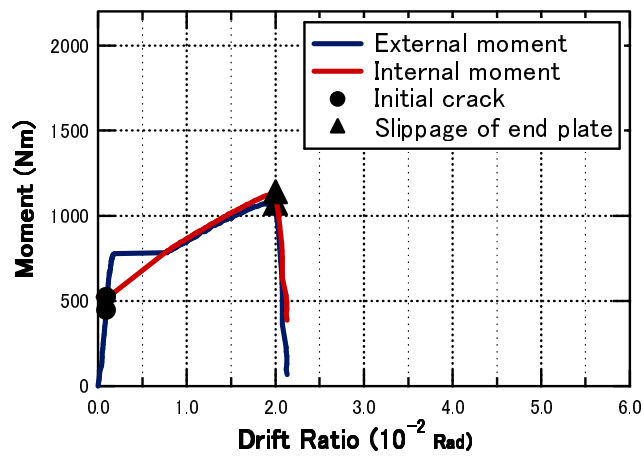
(a) SP at 2.1% drift ratio
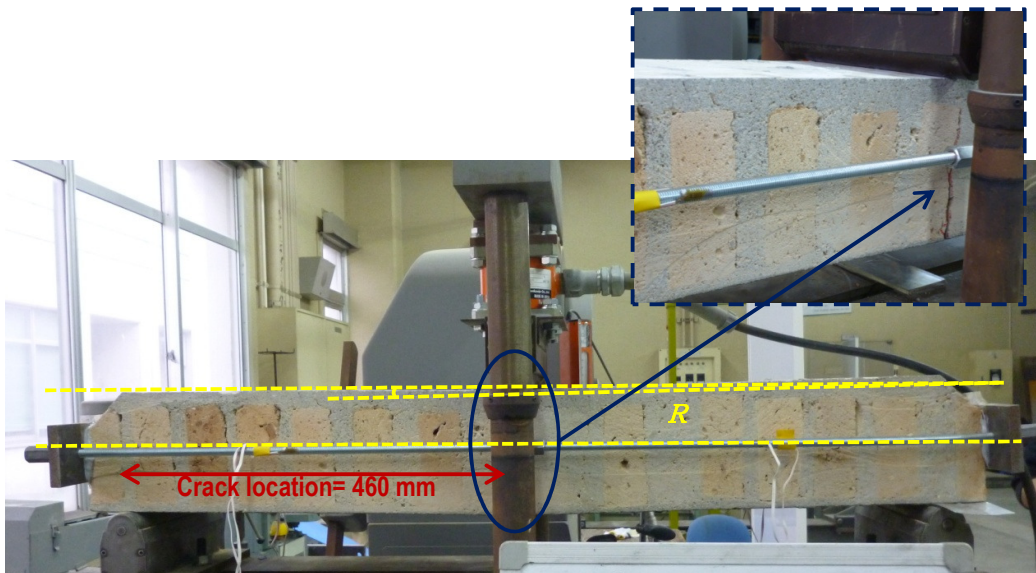
(b) SPI at 2.0% drift ratio

Photo A.2 Damage to specimens after/during loading

(a) SP specimen

(b)　　　　SPI specimen

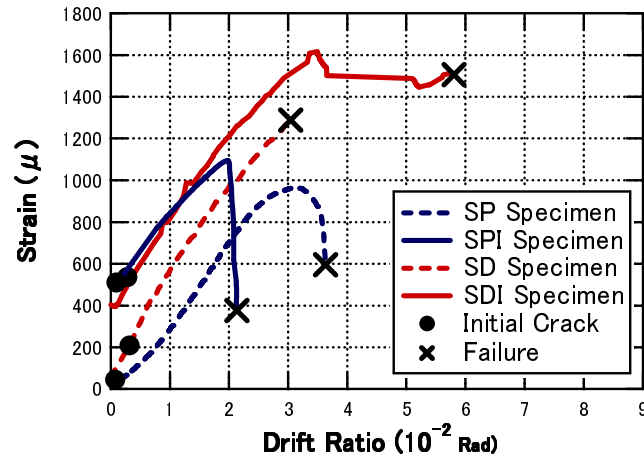Figure A.3 Moment-drift angle relationships of specimens

Figure A.4 Strain-drift angle relationships of strengthened specimens

Figure A.4 gives the averaged strain from gauges pasted on the rods of the strengthened specimens, versus drift angle relationships. Each tensile strain increased according to an increase of drift angle, which means that a higher compression acted on the cross-section under a larger drift angle. As a result, the higher resitances could be obtained under compression passibly induced by the proposed strengthning system.

Appendix B

Out-of-plane Performance of 2007 Sumatra Earthquake, Indonesia Brick Wall

A brick wall was extracted from the moderately damaged building after the 2007 Sumatera earthquakes and transported to Japan from Indonesia, as shown in Photo 5.1. Then, it was cut down to dimensions of 190 mm x 140 mm x 900 mm in width x thickness x height, as shown in Photo 5.2. Compressive strength in the longitudinal direction of the specimen was 2.91 N/mm^2.

Set-up of two displacement transducers for the test can be seen in Figure 5.4. They were located to measure the vertical displacements at the middle span of the specimen. The specimen was subjected to monotonic uniform distributed loading by the airbag.

Figure B.1 gives the relationship between vertical load and vertical deformation at the middle span which is the mean value from two transducers. The figure shows that

the specimen failed with the first cracking under a load of 1406 N at a small drift ratio (= vertical deformation / half-span of 450 mm) of 0.05% rad. Photo 5.5a shows the front view of the specimen after failure which indicated the specimen failed close to the middle span with the maximum bending moment along the wall height. The right vertical axis of the figure is the acceleration converted from the applied load as follows;

$$F = \frac{W}{G} A , \qquad So \quad A = \frac{F}{W} G \qquad\qquad (5.1)$$

where,

F: applied load = 1406 N

W: weight of specimen = 399 N

G: gravity acceleration = 9.8 m/s^2

A : equivalent acceleration, m/s^2

As a result, it was found that the specimen failed under an acceleration of 3.5 G. Although the height of specimen was 900 mm due to the limitation of transportation, as shown in Photo 5.2, the actual height of infill walls was 2750 mm. This means that the actual walls attain the maximum moment at the middle span and fail under an acceleration of 1.1 G (= 3.5G x 900 mm / 2750 mm), however, which was estimated under an assumption that walls are simply supported at both ends. The out-of-plane resistance of infill should be considered to accurately evaluate the seismic performance of the earthquake-damaged buildings considering infill effects nevertheless it was not considered in the previous investigation (Swe, Maidiawati and Sanada, 2011).
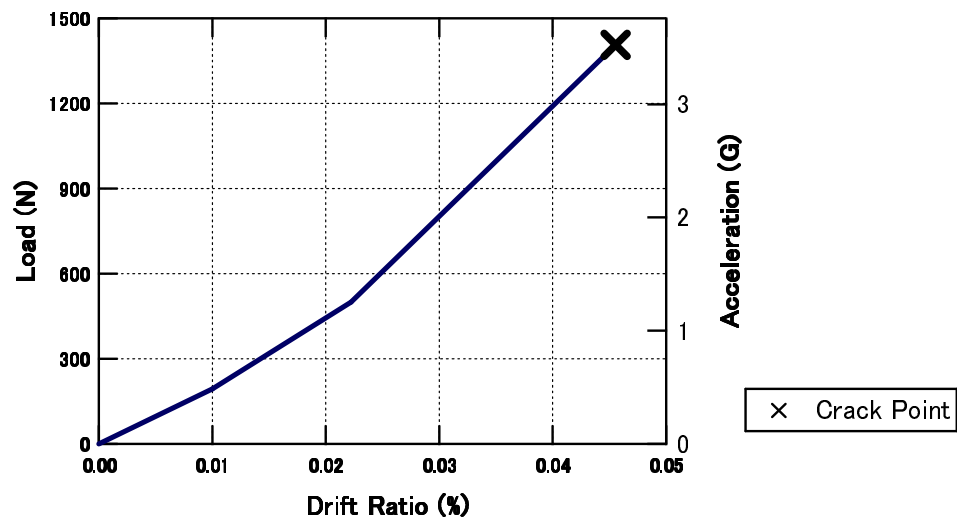
Figure B.1　　Loads - Drift relationship of unstrengthen brick masonry specimen

Publications

A.   Journal Papers with Referees' Review

1. Yulia Hayati, Yasushi Sanada, So Kasahara and Takuya Tomonaga, Developing a Test System for Evaluating Structural Performance of Masonry Walls under Out-of-Plane Uniform Loads, *AIJ Journal of Technology and Design,* Vol. 19 No. 42, 591-594, 2013.

2. Yulia Hayati and Yasushi Sanada, Out-Of-Plane Strengthening of Masonry Walls with Passive Compression, *AIJ Journal of Structural and Construction Engineering*, Vol. 79 No. 702, 1193-1201, 2014.

B.   International Conference with Referees' Review

1. Yulia Hayati, Yasushi Sanada, Takuya Tomonaga and Takafumi Kanada, Out-of-plane loading tests on masonry walls strengthened with restraining axial elongation, The Thirteenth East Asia-Pacific Conference on Structural Engineering and Construction (EASEC-13), Sapporo-Japan, 11-13 September, 2013.